Molecular Diversity (2022) 26:2595–2612
https://doi.org/10.1007/s11030-021-10347-8

ORIGINAL ARTICLE

Anthranilamides with quinoline and β-carboline scaffolds: design, synthesis, and biological activity

Maja Beus[1] · Leentje Persoons[2] · Dirk Daelemans[2] · Dominique Schols[2] · Kirsi Savijoki[3,4] · Pekka Varmanen[4] · Jari Yli-Kauhaluoma[5] · Kristina Pavić[1] · Branka Zorc[1]

Received: 9 June 2021 / Accepted: 2 November 2021 / Published online: 8 January 2022

Abstract

In the present study, we report the design and synthesis of novel amide-type hybrid molecules based on anthranilic acid and quinoline or β-carboline heterocyclic scaffolds. Three types of biological screenings were performed: (i) in vitro antiproliferative screening against a panel of solid tumor and leukemia cell lines, (ii) antiviral screening against several RNA viruses, and (iii) anti-quorum sensing screening using gram-negative *Chromobacterium violaceum* as the reporter strain. Antiproliferative screening revealed a high activity of several compounds. Anthranilamides **12** and **13** with chloroquine core and halogenated anthranilic acid were the most active agents toward diverse cancer cell lines such as glioblastoma, pancreatic adenocarcinoma, colorectal carcinoma, lung carcinoma, acute lymphoblastic, acute myeloid, chronic myeloid leukemia, and non-Hodgkin lymphoma, but also against noncancerous cell lines. Boc-protected analogs **2** and **3** showed moderate activities against the tested cancer cells without toxic effects against noncancerous cells. A nonhalogenated quinoline derivative **10** with *N*-benzylanthranilic acid residue was equally active as **12** and **13** and selective toward tumor cells. Chloroquine and quinoline anthranilamides **10**–**13** exerted pronounced antiviral effect against human coronaviruses 229E and OC43, whereas **12** and **13** against coronavirus OC43 (EC_{50} values in low micromolar range; selectivity indices from 4.6 to > 10.4). Anthranilamides **14** and **16** with PQ core inhibited HIV-1 with EC_{50} values of 9.3 and 14.1 μM, respectively. Compound **13** displayed significant anti-quorum/biofilm effect against the quorum sensing reporter strain (IC_{50} of 3.7 μM) with no apparent bactericidal effect.

✉ Branka Zorc
bzorc@pharma.hr

[1] Department of Medicinal Chemistry, Faculty of Pharmacy and Biochemistry, University of Zagreb, 10 000 Zagreb, Croatia

[2] Laboratory of Virology and Chemotherapy, Department of Microbiology, Immunology and Transplantation, KU Leuven, Rega Institute, 3000 Leuven, Belgium

[3] Drug Research Program, Division of Pharmaceutical Biosciences, University of Helsinki, 00014 Helsinki, Finland

[4] Department of Food and Nutrition, University of Helsinki, 00014 Helsinki, Finland

[5] Drug Research Program, Division of Pharmaceutical Chemistry and Technology, University of Helsinki, 00014 Helsinki, Finland

Graphical abstract

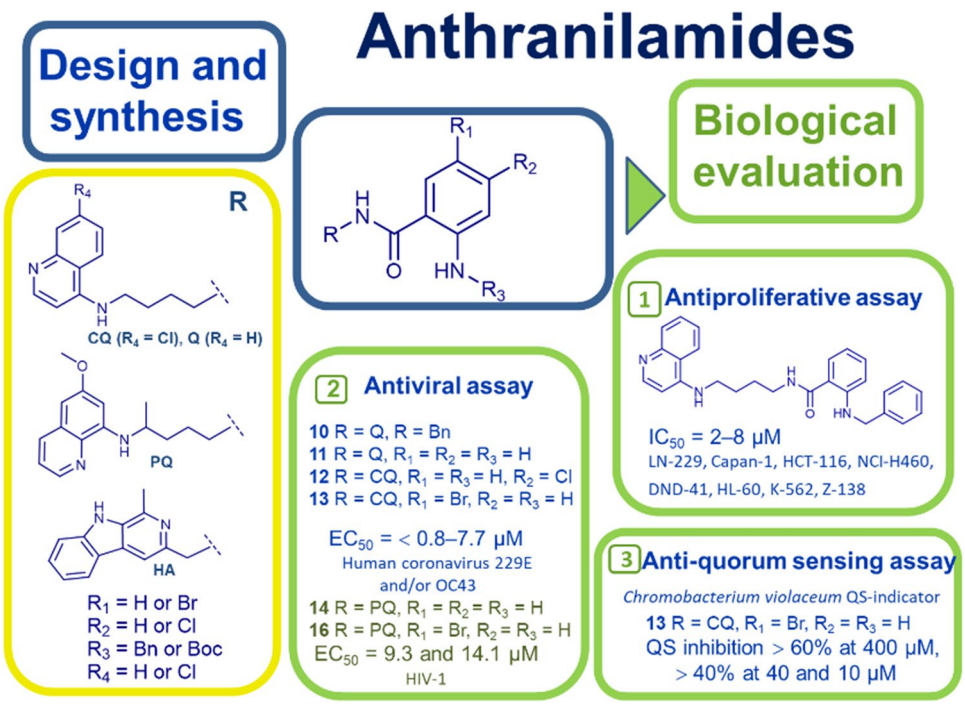

Keywords Anthranilamide · Quinoline · β-Carboline · Anticancer · Antiviral · Quorum sensing (QS) inhibition

Abbreviations

ADMA	Acetaldehyde dimethyl acetal
ADMP	2-Azido-1,3-dimethylimidazolinium hexafluorophosphate
ATR	Attenuated total reflection
Bn	Benzyl
Boc	*t*-Butoxycarbonyl
Capan-1	Pancreatic adenocarcinoma
CQ	N^1-(7-Chloroquinolin-4-yl) butane-1,4-diamine
DBU	1,8-Diazabicyclo[5.4.0]undec-7-ene
DIEA	*N,N*-Diisopropylethylamine
DND-41	Acute lymphoblastic leukemia
HA	(1-Methyl-9*H*-pyrido[3,4-*b*]indol-3-yl) methanamine
HATU	1-[Bis(dimethylamino)methylene]-1*H*-1,2,3-triazolo[4,5-*b*]pyridinium 3-oxid hexafluorophosphate
HCT-116	Colorectal carcinoma
HEL 299	Human lung fibroblasts
Hep-2	Human epithelial type 2 cell
HHQ	2-Heptylquinolin-4(1*H*)-one
HL-60	Acute myeloid leukemia
K-562	Chronic myeloid leukemia
LN-229	Glioblastoma
MDCK	Madin–Darby canine kidney cells
MTS	3-(4,5-Dimethylthiazol-2-yl)-5-(3-carboxymethoxyphenyl)-2-(4-sulfophenyl)-2*H*-tetrazolium
NCI-H460	Lung carcinoma
PMPA	2-Phosphonomethoxypropyl adenine
PQ	Primaquine
PQS	2-Heptyl-3-hydroxyquinolin-4(1*H*)-one
Q	Quinoline
QS	Quorum sensing
T3P	Propanephosphonic acid anhydride
TEA	Trimethylamine
Z-138	Non-Hodgkin lymphoma

Introduction

Anthranilic acid (2-aminobenzoic acid) is an aromatic non-peptide-forming amino acid. It is a biosynthetic precursor of tryptophan and the initial building block in the biosynthesis of *Pseudomonas* quinolone signal PQS (2-heptyl-3-hydroxy-quinolin-4(1*H*)-one) and its precursor HHQ (2-heptylquinolin-4(1*H*)-one) [1]. It is also a motive present in several drugs and insecticides (Fig. 1) [2, 3].

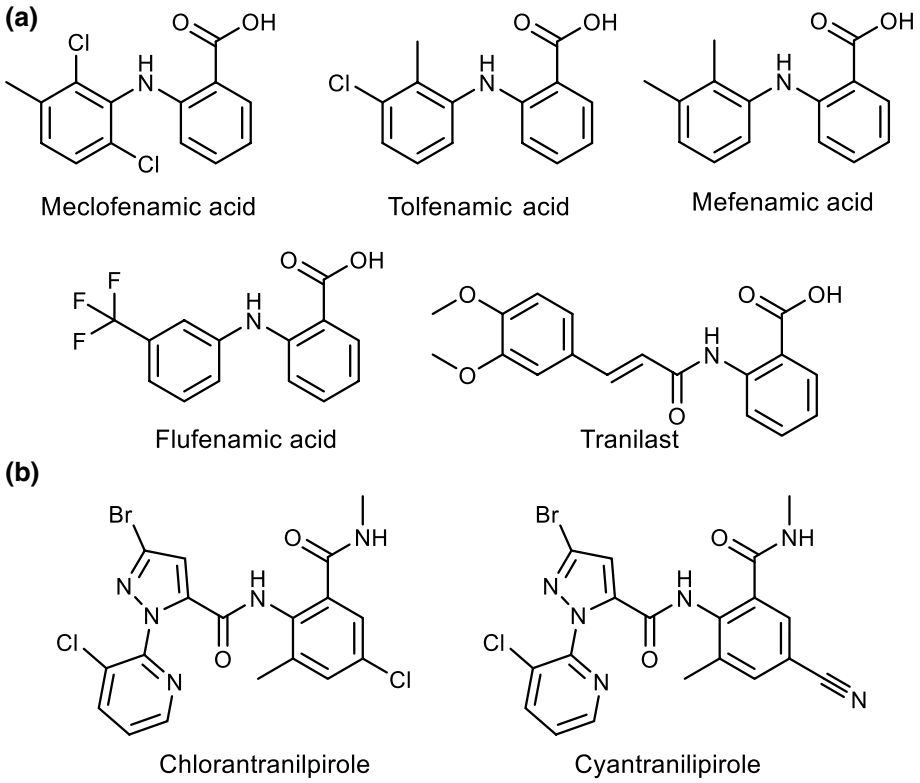

Fig. 1 Drugs **a** and insecticides **b** based on anthranilic acid

Tranilast was first approved for the therapy of bronchial asthma and later for the treatment of keloids and hypertrophic scars [4]. It suppresses the proliferation of fibroblasts and decreases the viability of various cancer cell lines, along with the promotion of apoptosis, inhibition of angiogenesis, and cell migration [5–9]. These findings prompted us to design novel anthranilic acid-based hybrids as potential anticancer agents. To design compounds with improved activity, we combined anthranilic acid motif with other two scaffolds known for their antiproliferative properties, namely quinoline and β-carboline. Considering the numerous preclinical and clinical trials confirming the usefulness of antimalarial drugs in cancer therapy [10–16] and based on our previous experience with primaquine (PQ) and chloroquine derivatives with pronounced antiproliferative activities [17, 18], we have chosen N^1-(7-chloroquinolin-4-yl)butane-1,4-diamine (CQ), as a simplified chloroquine molecule, and PQ-base as amino components for the preparation of anthranilamides. On the other hand, β-carboline alkaloids (harmane, harmine, and harmaline) possess diverse biological activities, including antimalarial and antiproliferative activity [19–37]. Zhao et al. investigated the cytotoxic activity of β-carboline conjugates with amino acid esters and found aromatic (Phe) and basic amino acid derivatives (Lys and Arg) as the most active against several cancer cell lines [38]. This finding further corroborated the idea to combine β-carboline and anthranilic acid moieties in hybrid molecules.

Chloroquine is also known for its antiviral effects [39–41]. During the COVID-19 pandemic, its antiviral potential was investigated intensively. A number of scientific papers reported chloroquine efficacy and acceptable safety in the treatment of COVID-19 associated pneumonia [42–46]. Several clinical trials based on chloroquine started as well, although some of them were discontinued due to the lack of clinical efficacy [47]. Since the antiviral effects of harmala alkaloids were also reported [48–52], the aim of the present study was to design and prepare a series of anthranilamides with quinoline and β-carboline cores and explore their antiproliferative and antiviral potential. Some quinoline derivatives, including chloroquine-based fumardiamides prepared by our research group, were previously shown to prevent cell-to-cell communication (i.e., quorum sensing, QS), expression of virulence factors, and biofilm formation in gram-negative pathogens [53, 54]. Based on these findings, we additionally evaluated potential of the novel quinoline derivatives as QS inhibitors.

Results and discussion

Chemistry

A series of anthranilamides **11–19** with quinoline- or harmane-based amines and their *N*-protected precursors **1–10**

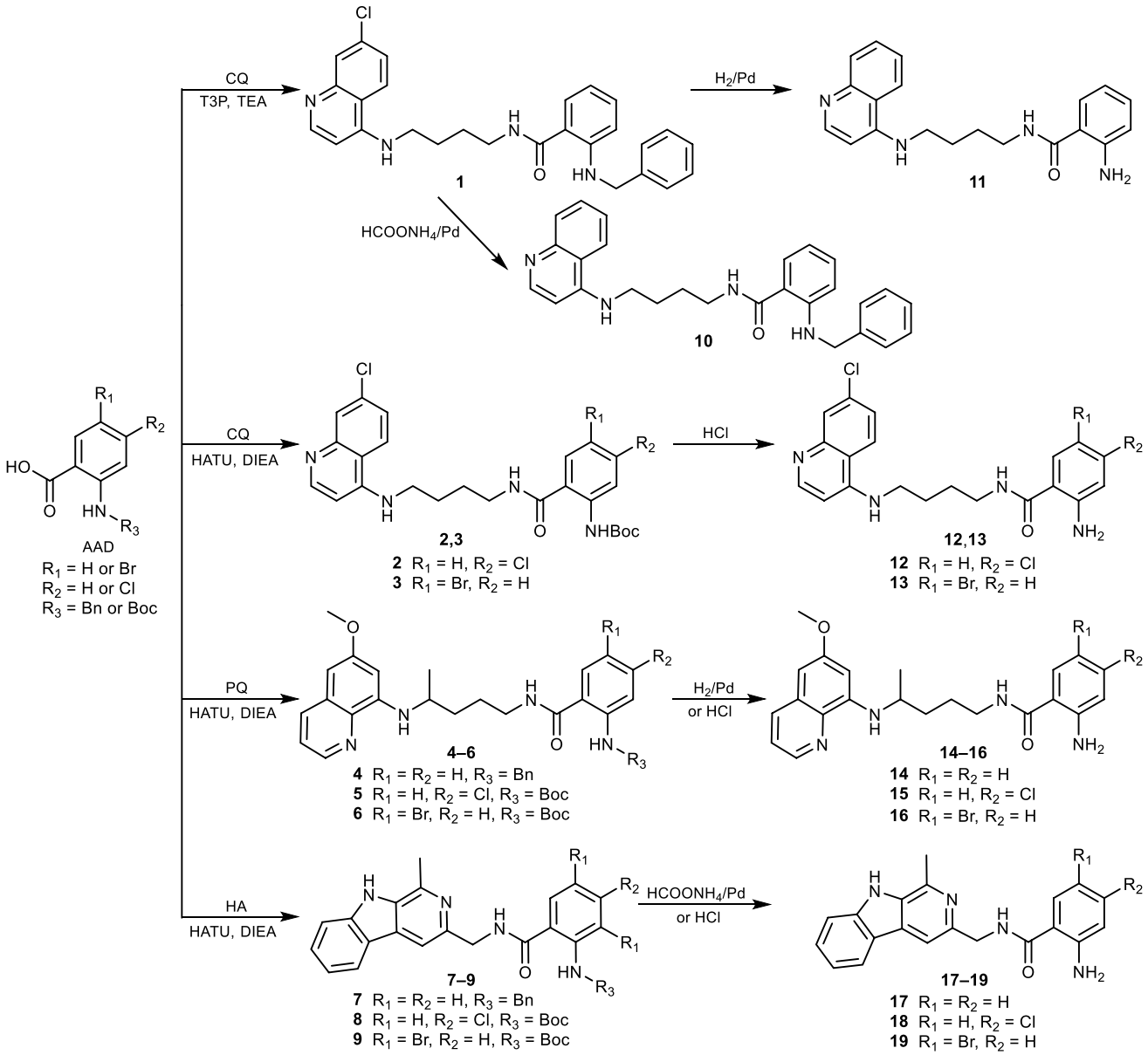

Scheme 1 Synthetic route for the preparation of anthranilamides **1**–**19**

were prepared. The synthetic routes leading to the title compounds are outlined in Scheme 1.

The first step included the coupling of *N*-protected anthranilic acid (*N*-benzylanthranilic acid, *N*-Boc-4-chloroanthranilic acid or *N*-Boc-5-bromoanthranilic acid) with corresponding amines: N^1-(7-chloroquinolin-4-yl)butane-1,4-diamine (CQ), primaquine (PQ) or harmane-based amine (1-methyl-9*H*-pyrido[3,4-*b*]indol-3-yl)methanamine (HA). *N*-protected anthranilic acids are commercially available compounds, whereas the starting amines were prepared following the published procedures. N^1-(7-chloroquinolin-4-yl)butane-1,4-diamine was obtained from 4,7-dichloroquinoline and 1,4-diaminobutane under microwave irradiation (300 W) at 95 °C [17] and PQ was prepared from PQ diphosphate. The preparation of the aminoharmane derivative HA was more complex. The harmane scaffold was built from tryptophan ester utilizing a microwave-assisted Pictet–Spengler reaction [38, 55, 56]. Briefly, methyl 3-(1*H*-indol-3-yl)-2-aminopropanoate, acetaldehyde dimethyl acetal (ADMA), and trifluoroacetic acid (TFA) were heated under microwave irradiation to afford a corresponding tetrahydro-β-carboline product, which was then aromatized using $KMnO_4$ at room temperature. Further steps included: (i) reduction of the harmane ester to alcohol using $LiAlH_4$, (ii) conversion of the alcohol to azide by means of 2-azido-1,3-dimethylimidazolinium hexafluorophosphate (ADMP)

and 1,8-diazabicyclo[5.4.0]undec-7-ene (DBU), and finally, (iii) reduction of the azide to amine HA under a hydrogen atmosphere.

Compound **1** was prepared by coupling of *N*-benzylanthranilic acid with CQ utilizing propanephosphonic acid anhydride (T3P) and triethylamine (TEA), whereas *N*-protected anthranilamides **2**–**9** were obtained by coupling of the corresponding anthranilic acid derivative with CQ, PQ or HA using 1-[bis(dimethylamino)methylene]-1*H*-1,2,3-triazolo[4,5-*b*]pyridinium 3-oxid hexafluorophosphate (HATU)/*N,N*-diisopropylethylamine (DIEA) coupling system.

The deprotection of compound **1** with ammonium formate/Pd was rather unexpected and afforded product **10**, still bearing benzyl group, but without chlorine in the quinoline part of the molecule. On the other hand, hydrogenation of compound **1** with Pd catalyst gave deprotected quinoline (Q) derivative **11** without chlorine atom. The removal of the Boc-group from compounds **2**, **3**, **5**, **6**, **8**, and **9** proceeded smoothly with HCl and so did the removal of the benzyl (Bn) group from **4** and **7** using H_2/Pd and $HCOONH_4$/Pd, respectively. Altogether, one Q-derivative, two CQ, three PQ, and three HA anthranilamides with free amino groups were prepared.

A common set of physicochemical parameters (molecular weight, partition coefficient, number of H-bond donors and acceptors, molecular refractivity, topological polar surface area, rotatable bonds count) was calculated using Chemicalize.org software and is presented in Table 1 [57]. Compounds **7**–**19** are fully in agreement with Lipinski's and Gelovani's rules for prospective small molecular drugs (MW ≤ 500, log $P \leq 5$, number of H-bond donors ≤ 5, number of H-bond acceptors ≤ 10, TPSA < 140 Å^2, MR within the range of 40 and 130 cm^3/mol, the number of atoms 20–70), while **1**–**6** show slight deviations in MR, MW and/or log *P*.

Antiproliferative activity

Our first goal was to evaluate the anticancer activity of newly prepared quinoline- and harmane-based anthranilamides against a series of cancer cell lines. In vitro experiments on eight human solid tumor and leukemia cell lines (glioblastoma LN-229, pancreatic adenocarcinoma Capan-1, colorectal carcinoma HCT-116, lung carcinoma NCI-H460, acute lymphoblastic leukemia DND-41, acute myeloid leukemia HL-60, chronic myeloid leukemia K-562, and non-Hodgkin lymphoma Z-138) were performed. Normal human lung fibroblasts (HEL 299) were used as a model for noncancerous cells. The cells were treated with compounds at different concentrations and the IC_{50} values were determined (Table 2). Docetaxel (DTX) and staurosporine (STS) were

Table 1 The Lipinski and Gelovani parameters of the anthranilamides **10**–**19** calculated with Chemicalize.org program [57]

Cmpd	Molecular formula	Number of atoms	MW	log *P*	HBD	HBA	MR (cm^3 mol^{-1})	TPSA (Å^2)	RBC
1	$C_{27}H_{27}ClN_4O$	60	458.99	5.51	3	4	137.36	66.05	10
2	$C_{25}H_{28}Cl_2N_4O_3$	62	503.42	5.18	3	5	137.65	92.35	10
3	$C_{25}H_{28}BrClN_4O_3$	62	547.88	5.34	3	5	140.47	92.35	10
4	$C_{29}H_{32}N_4O_2$	67	468.60	5.16	3	5	143.44	75.28	11
5	$C_{27}H_{33}ClN_4O_4$	69	513.04	4.83	3	6	143.73	101.58	11
6	$C_{27}H_{33}BrN_4O_4$	69	557.49	5.00	3	6	146.54	101.58	11
7	$C_{27}H_{24}N_4O$	56	420.52	4.73	3	3	128.78	69.81	6
8	$C_{25}H_{25}ClN_4O_3$	58	464.95	4.40	3	4	129.07	96.11	6
9	$C_{25}H_{25}BrN_4O_3$	58	509.40	4.57	3	4	131.89	96.11	6
10	$C_{27}H_{28}N_4O$	60	424.55	4.90	3	4	132.55	66.05	10
11	$C_{20}H_{22}N_4O$	47	334.423	2.88	3	4	102.45	80.04	7
12	$C_{20}H_{20}Cl_2N_4O$	47	403.310	4.09	3	4	112.06	80.04	7
13	$C_{20}H_{20}BrClN_4O$	47	447.760	4.25	3	4	114.88	80.04	7
14	$C_{22}H_{26}N_4O_2$	54	378.476	3.14	3	5	113.33	89.27	8
15	$C_{22}H_{25}ClN_4O_2$	54	412.920	3.74	3	5	118.13	89.27	8
16	$C_{22}H_{25}BrN_4O_2$	54	457.372	3.91	3	5	120.95	89.27	8
17	$C_{20}H_{18}N_4O$	43	330.391	2.71	3	3	98.67	83.80	3
18	$C_{20}H_{17}ClN_4O$	43	364.830	3.31	3	3	103.48	83.80	3
19	$C_{20}H_{17}BrN_4$	43	409.287	3.48	3	3	106.30	83.80	3

MW, molecular weight; log *P*, partition coefficient; HBD, H-bond donor; HBA, H-bond acceptor; MR, molecular refractivity; TPSA, topological polar surface area; RBC, rotatable bond counts

Table 2 Antiproliferative screening of anthranilamides **1–19** toward human cancer cell lines

Cmpd	Structural formula	IC_{50} (μM)[a]								
		LN-229	Capan-1	HCT-116	NCI-H460	DND-41	HL-60	K-562	Z-138	HEL 299
1	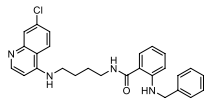	53.5 ± 12.2	57.6 ± 14.6	> 100	> 100	> 100	> 100	55.7 ± 10.0	> 100	8.0 ± 4.4
2	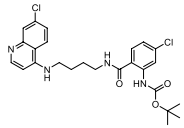	30.1 ± 2.1	20.4 ± 9.0	32.4 ± 20.0	21.2 ± 10.0	46.2 ± 1.9	41.5 ± 17.0	54.5 ± 18.5	28.6 ± 14.6	> 100
3	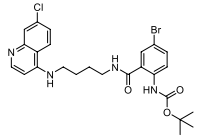	48.4 ± 20.0	40.6 ± 4.2	66.1 ± 30.0	69.3 ± 30.7	51.3 ± 4.4	60.5 ± 17.0	51.2 ± 9.3	55.2 ± 9.2	> 100
4	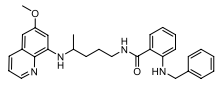	> 100	> 100	> 100	> 100	> 100	> 100	> 100	> 100	> 100
5	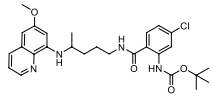	> 100	> 100	> 100	> 100	> 100	> 100	> 100	> 100	> 100
6	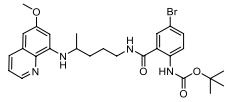	> 100	> 100	> 100	> 100	> 100	> 100	> 100	> 100	> 100
7	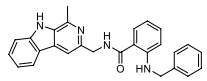	35.8 ± 9.3	27.5 ± 8.1	34.6 ± 6.0	28.4 ± 4.0	53.5 ± 6.7	66.2 ± 18.3	90.7 ± 18.5	21.0 ± 10.1	50.9 ± 2.7
8	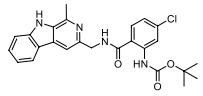	20.8 ± 13.8	6.5 ± 2.9	28.9 ± 24.1	8.3 ± 4.3	32.1 ± 20.8	6.7 ± 0.2	29.1 ± 21.3	8.2 ± 1.9	7.1 ± 1.8
9	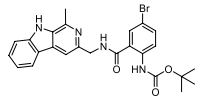	8.3 ± 3.1	5.8 ± 3.0	32.9 ± 7.9	3.2 ± 1.8	12.5 ± 6.9	10.8 ± 3.3	63.1 ± 36.9	4.1 ± 1.8	7.5 ± 1.0
10	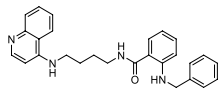	3.0 ± 2.0	4.2 ± 3.4	7.4 ± 1.5	2.2 ± 0.8	8.0 ± 3.2	14.9 ± 7.3	5.9 ± 3.5	4.6 ± 2.0	33.6 ± 15.6

Table 2 (continued)

Cmpd	Structural formula	IC_{50} (μM)[a]								
		LN-229	Capan-1	HCT-116	NCI-H460	DND-41	HL-60	K-562	Z-138	HEL 299
11	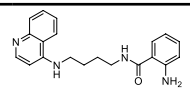	39.7 ± 4.4	62.2 ± 9.7	45.4 ± 4.9	87.4 ± 12.6	59.6 ± 1.7	44.7 ± 11.0	18.7 ± 6.7	31.2 ± 1.1	41.6 ± 1.2
12	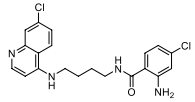	2.8 ± 1.2	6.3 ± 2.8	8.9 ± 3.0	7.3 ± 1.5	9.2 ± 2.2	9.8 ± 3.5	8.4 ± 3.2	7.2 ± 2.6	7.4 ± 1.2
13	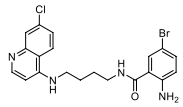	3.1 ± 0.8	5.4 ± 1.8	7.0 ± 0.3	5.3 ± 0.4	7.8 ± 4.1	10.3 ± 3.2	7.7 ± 1.1	6.0 ± 2.6	7.8 ± 1.8
14	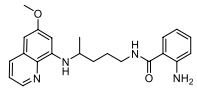	> 100	> 100	> 100	76.7 ± 25.0	> 100	> 100	> 100	> 100	> 100
15	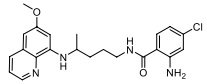	> 100	> 100	> 100	> 100	> 100	> 100	> 100	> 100	> 100
16	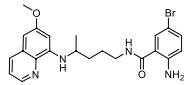	> 100	> 100	> 100	> 100	> 100	> 100	> 100	> 100	> 100
17	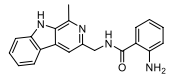	41.0 ± 0.3	31.4 ± 1.9	48.4 ± 3.8	54.8 ± 5.9	61.5 ± 2.1	44.0 ± 8.4	52.0 ± 5.3	35.1 ± 4.5	32.8 ± 3.3
18	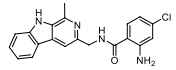	44.0 ± 7.6	56.3 ± 24.1	55.0 ± 17.7	43.8 ± 8.4	> 100	> 100	> 100	> 100	> 100
19	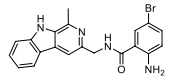	46.2 ± 7.5	38.9 ± 5.8	60.8 ± 31.0	55.0 ± 5.0	68.3 ± 12.2	66.3 ± 34.0	64.9 ± 4.9	55.5 ± 12.1	82.6 ± 17.4
CQ		8.9 ± 2.3	46.1 ± 1.3	65.5 ± 7.3	> 100	59.5 ± 3.5	> 100	50.6 ± 2.9	47.4 ± 5.3	84.7 ± 15.3
PQ		45.4 ± 1.2	45.6 ± 3.5	53.9 ± 4.2	> 100	50.2 ± 16.7	28.4 ± 1.6	40.5 ± 6.0	11.4 ± 1.1	> 100
HA		> 100	68.6 ± 3.4	> 100	85.1 ± 14.8	> 100	> 100	> 100	57.4 ± 32.6	> 100
DTX[b]		1.8 ± 3.0	10.0 ± 3.0	2.5 ± 3.0	27.1 ± 3.0	5.5 ± 3.0	13.7 ± 3.0	8.9 ± 3.0	2.5 ± 3.0	nt
STS[b]		51.1 ± 3.0	38.2 ± 3.0	68.7 ± 3.0	38.4 ± 3.0	40.7 ± 3.0	59.8 ± 3.0	73.9 ± 3.0	40.7 ± 3.0	nt

[a]IC_{50}, the concentration required to decrease viability or cell growth by 50%; CQ, chloroquine, PQ, primaquine; HA, aminoharmane, DTX, docetaxel, STS, staurosporine

[b]Concentration in nM

included as positive controls. All anthranilamides with PQ core (**4**–**6**, **14**–**16**) were inactive. In the CQ series, compounds with the free amino group were more active than their *N*-protected analogues pairs, suggesting the importance of amino moiety for activity. CQ derivatives **12** and **13** with two halogen atoms (chlorine in amine part and chlorine or bromine atoms in the carboxylic part of the molecules) and free amino group exerted the highest antiproliferative activity with IC_{50} between 2 and 10 µM, approximately ten times lower than the parent compound and the analogous compounds **1**–**3** with *N*-protected amino groups. However, these compounds exerted high antiproliferative activity against HEL 299 cells as well. On the other hand, Boc-protected analogues **2** and **3** showed moderate activities against tested cancer cells and no cytotoxicity against noncancerous cells. *N*-benzyl-protected quinoline derivative **10** without halogen substituents was equally active as compounds **12** and **13**, whereas its analogue **11** with a free amino group had approximately 3–40 lower activity, depending on the cell type. Compound **10** showed favorable selectivity, ranging from 2 to 10 depending on the cell type. Comparison of *N*-protected CQ derivatives **1**–**3** with PQ derivatives **4**–**6** and HA derivatives **7**–**9** revealed the importance of the heterocycle part of the molecule. IC_{50} values of the most effective HA derivatives **8** and **9** were in the low micromolar range against four tested cancer cell types, but also against HEL 299. Within all tested anthranilamides, 2-(benzylamino)-*N*-[4-(quinolin-4-ylamino)butyl]benzamide (**10**) is the most promising compound with the best toxicity/activity ratio.

Antiviral activity

In addition, the synthesized anthranilamides were evaluated against a broad variety of viruses including HIV-1 NL4.3 and HIV-2 ROD, influenza A/H1N1 A/Ned/378/05, influenza A/H3N2 A/HK/7/87, influenza B B/Ned/537/05, respiratory syncytial virus and human coronaviruses 229E and OC43 (in MT-4, MDCK, Hep-2 or HEL 299 cells; positive controls: PMPA, AMD3100, zanamivir, ribavirin, rimantadine, ribavirin, DS-10.000, remdesivir, and GS-441524, respectively). Chloroquine and quinoline anthranilamides **10**–**13** exerted pronounced antiviral effect against human coronavirus 229E and two of them, **12** and **13**, against coronavirus OC43 as well, with EC_{50} values (50% effective concentrations) in the low micromolar range (< 0.8–7.7 µM), comparable with chloroquine's EC_{50}. Their selectivity indices (CC_{50} to EC_{50} ratio, SI) varied from 4.6 to > 10.4, while chloroquine SI was higher (approximately 30). PQ and HA derivatives were inactive against coronaviruses. Anthranilamide **14** and bromoanthranilamide **16** with PQ core were able to inhibit HIV-1 with EC_{50} values of 9.3 and 14.1 µM, respectively, yielding a favorable selectivity index of 8.4 for **14**. Primaquine itself showed no anti-HIV activity. Although chloroquine shows selective antiviral activity against both HIV-1 and HIV-2, none of the anthranilamides with CQ core showed antiretroviral activity. Also, influenza viruses and the respiratory syncytial virus did not respond to any of the anthranilamides tested. All compounds were tested, but only selected results are presented in Tables 3 and 4.

Table 3 Antiviral activity of selected anthranilamides against human coronaviruses 229E and OC43

Cmpd	Cytotoxicity (CC_{50})	Antiviral activity (EC_{50})			
		229E	SI	OC43	SI
10	5.6 ± 3.0	< 0.8	> 7	> 100	–
11	46.3 ± 1.2	7.7 ± 0.3	6.0	> 100	–
12	8.3 ± 0.78	1.8 ± 1.2	4.6	< 0.8	> 10.4
13	7.5 ± 1.3	1.4 ± 0.1	5.4	1.5 ± 0.2	5.0
CQ	40.8 ± 2.2	1.4 ± 0.2	29.1	1.3 ± 1.2	31.4
PQ	> 100	> 100	–	> 100	–
HA	> 100	> 100	–	> 1002	–
Remdesivir	> 10	0.06 ± 0.02	> 160	0.04 ± 0.01	> 250
GS-441524	> 100	0.9 ± 0.1	> 110	1.3 ± 0.1	> 75

In HEL cell culture; CC_{50} (µM), 50% cytotoxic concentration, as determined by measuring the cell viability with the colorimetric formazan-based MTS assay; EC_{50} (µM), concentration producing 50% inhibition of virus-induced cytopathic effect, as determined by measuring the cell viability with the colorimetric formazan-based MTS assay; SI, selectivity index (CC_{50} to EC_{50} ratio); CQ, chloroquine, PQ, primaquine; HA, aminoharman; GS-441524, main plasma metabolite of remdesivir

Table 4 Antiviral activity of selected anthranilamides against HIV-1 and HIV-2

Cmpd	Cytotoxicity (CC_{50})	Antiviral activity (EC_{50})			
		HIV-1 NL4.3	SI	HIV-2 ROD	SI
14	78.2 ± 9.3	9.3 ± 0.5	8.4	> 100	–
16	56.4 ± 1.6	14.1 ± 0.6	4.0	> 100	–
CQ	> 100	31.7 ± 4.7	> 3.2	3.8 ± 1.6	> 26.3
PQ	17.9 ± 8.0	> 100	–	> 100	–
HA	22.3 ± 4.9	> 100	–	> 100	–
PMPA	> 100	1.6	> 64	0.6	> 161

In MT-4 cell culture; CC_{50} (µM), 50% cytotoxic concentration; EC_{50} (µM), concentration producing 50% inhibition of virus-induced cytopathic effect; SI, selectivity index (CC_{50} to EC_{50} ratio); CQ, chloroquine, PQ, primaquine; HA, aminoharman; PMPA, 2-phosphonomethoxypropyl adenine [58]

Anti-QS and bactericidal effects on the *Chromobacterium violaceum* QS-reporter strain

Anthranilamides **1**–**19** were also tested for their ability to prevent the induction of QS and the following biofilm

formation in gram-negative bacteria using *C. violaceum* ATCC31532 as the QS-indicator strain [59]. Three compounds, **11**, **12**, and **13**, displayed significant anti-QS effect (> 34–63%) against the reporter strain with similar or minor (≤ 32%) bactericidal effect at 400 µM level under the screening conditions used (Fig. 2, SI Table 1).

Compound **13** with IC_{50} of 3.7 µM (95% CI 0.4–10.3) was the most active: At 400 µM concentration, the compound reduced the QS-induced violacein production in *C. violaceum* by more than 60%, while the viability of the reporter strain was less affected (ca., 30% reduction) under the same conditions. This compound showed reasonably high anti-QS activity (> 40%) with no apparent bactericidal effect on the reporter also at 40 and 10 µM concentration levels.

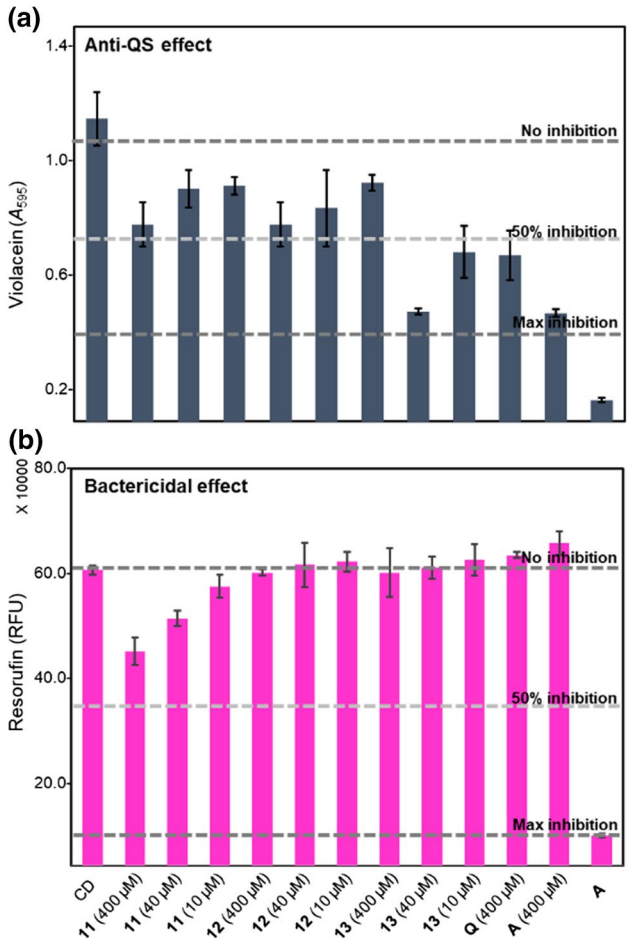

Fig. 2 Three anthranilamide derivatives showed high anti-QS activity against the *C. violaceum* ATCC31532 QS-reporter strain. The selected compounds were tested at 400, 40 and 10 µM concentration levels and their effects on the violacein production (**a**) and viability (**b**) were recorded after an overnight incubation at 27 °C. CD, cells with 2% DMSO; A, azithromycin; Q, quercetin (both at 400 µM). Violacein production was monitored at 595 nm and the reduction of resazurin to resorufin with $\lambda = 560/590$ nm using the PerkinElmer Victor3 multilabel plate reader. The experiment was repeated three times. Error bars, ± SD ($n = 3$)

Interfering with the bacterial QS signaling is considered a method of choice to combat pathogenic biofilms and recalcitrant infections without increasing the risk of resistance development [60]. Thus, from all tested compounds, **13** shows promise as a potentially new anti-QS agent capable of preventing biofilm formation of gram-negative pathogens without posing selective pressure on the bacterial cell.

Conclusions

In conclusion, we have successfully prepared and characterized 19 novel anthranilamides with different heterocycle and anthranilic acid moieties and evaluated their potential as antiproliferative and antiviral agents. Of all tested anthranilamides, 2-(benzylamino)-*N*-[4-(quinolin-4-ylamino) butyl]benzamide (**10**) was the most promising compound with the best selectivity index. Several anthranilamides with CQ, Q and HA cores showed high antiproliferative activities against all or selected cancer cells, but also general toxicity, whereas two compounds exerted moderate, but selective activity toward cancer cell lines. Chloroquine and quinoline anthranilamides **10**–**13** exerted pronounced antiviral effect against human coronavirus 229E and two of them, **12** and **13**, also against coronavirus OC43. Quinoline anthranilamide **13** displayed significant anti-QS/-biofilm activity in gram-negative QS-reporter strain, while primaquine anthranilamide **14** showed favorable selectivity against HIV-1. Taken together, obtained results could serve as a basis for the development of lead compounds with high and selective antitumor and/or antiviral/antibacterial properties.

Experimental

Materials and methods

Melting points were determined on the SMP3 apparatus (Barloworld Scientific, UK) in open capillaries and are uncorrected. CEM Discover microwave reactor was used for microwave reactions (CEM GmbH, Germany). IR spectra were recorded on Spectrum One (PerkinElmer, UK) and UV–VIS spectra on Lambda 20 double-beam spectrophotometers (PerkinElmer, UK). NMR ^{1}H and ^{13}C spectra were recorded at 25 °C on the NMR Avance 600 spectrometer (Bruker, Germany) at 300.13 or 600.13 and 75.47 or 150.9 MHz for ^{1}H and ^{13}C nuclei, respectively. Chemical shifts (δ) are reported in parts per million (ppm) relative to tetramethylsilane in the ^{1}H and the dimethyl sulfoxide (DMSO) residual peak as a reference in the ^{13}C spectra (39.51 ppm). Coupling constants (J) are reported in hertz (Hz). Mass spectra were collected on an HPLC–MS/MS instrument (HPLC, Agilent Technologies 1200 Series; MS,

Agilent Technologies 6410 Triple Quad) using electrospray ionization in positive mode. Elemental analyses were performed on a CHNS LECO analyzer (LECO Corporation, USA). All compounds were routinely checked by TLC with Merck silica gel 60F-254 glass plates using dichloromethane/methanol 9.5:0.5, 9:1, 8.5:1.5, cyclohexane/ethyl acetate 1:1 and cyclohexane/ethyl acetate/methanol 3:1:0.5, 1:1:0.5 as the solvent systems. Spots were visualized by short-wave UV light and iodine vapor. Column chromatography was performed on silica gel 0.063–0.200 mm (Sigma-Aldrich, USA) with the same eluents used in TLC.

All chemicals and solvents were of analytical grade and purchased from commercial sources. 4,7-Dichloroquinoline, butane-1,4-diamine, acetaldehyde dimethyl acetal (ADMA), 1,8-diazabicyclo[5.4.0]undec-7-ene (DBU), lithium aluminum hydride, palladium on activated charcoal, propanephosphonic acid anhydride (T3P), ammonium formate, triethylamine (TEA), DIEA, and HATU were purchased from Sigma-Aldrich. *N*-Boc-4-chloroanthranilic acid and *N*-Boc-5-bromoanthranilic acid were purchased from Fluorochem. *N*-Benzylanthranilic acid, 2-azido-1,3-dimethylimidazolinium hexafluorophosphate (ADMP) and L-tryptophan methyl ester hydrochloride were purchased from TCI. Potassium permanganate was purchased from Gram-Mol and hydrochloric acid from Carlo Erba. Anhydrous solvents were dried and redistilled prior to use. PQ was prepared from PQ diphosphate. All reactions with PQ were run protected from light.

Syntheses

2-(Benzylamino)-N-{4-[(7-chloroquinolin-4-yl)amino]butyl}benzamide (1) To a mixture of N^1-(7-chloroquinolin-4-yl)butane-1,4-diamine (0.067 g, 0.27 mmol), *N*-benzylanthranilic acid (0.067 g, 0.297 mmol) and TEA (0.055 g, 0.54 mmol) in *N*,*N*-dimethylformamide (DMF, 1 mL) was added dropwise a 50% solution of T3P in EtOAc (160 µL, 0.27 mmol) at 0 °C. The reaction mixture was slowly allowed to warm to r.t. and stirred for 19 h. The reaction mixture was diluted with EtOAc and extracted with a 5% solution of NaOH in water (3 × 30 mL) and washed with water (1 × 30 mL). The organic layer was dried through phase separator, filtrated, and evaporated under reduced pressure. After purification by column chromatography (mobile phase dichloromethane/methanol 9:1) and crystallization from diethyl ether, 0.082 g (66%) of white solid **1** was obtained; mp 102–104 °C; IR (KBr) (ν_{max}/cm^{-1}): 3284, 3032, 2934, 1623, 1578, 1535, 1449, 1426, 1368, 1352, 1328, 1279, 1245, 1202, 1159, 1136, 1064, 910, 871, 806, 747, 695, 499; ^{1}H NMR (δ/ppm): 8.38–8.35 (m, 2H), 8.28 (d, 1H, J = 9.1 Hz), 8.23 (t, 1H, J = 5.7 Hz), 7.78 (d, 1H, J = 2.2 Hz), 7.54 (dd, 1H, J = 7.8, 1.3 Hz), 7.43 (dd, 1H, J = 9.0, 2.2 Hz), 7.35–7.28 (m, 5H), 7.26–7.16 (m, 2H), 6.62 (d, 1H, J = 8.2 Hz), 6.55 (t, 1H, J = 7.4 Hz), 6.48 (d, 1H, J = 5.5 Hz), 4.36 (d, 2H, J = 5.8 Hz), 3.32–3.26 (m, 4H), 1.75–1.60 (m, 4H); ^{13}C NMR (δ/ppm): 169.10, 151.90, 150.05, 149.12, 148.93, 139.57, 133.31, 132.24, 128.44, 128.23, 127.48, 127.10, 126.82, 124.09, 123.94, 117.45, 115.47, 114.38, 111.45, 98.64, 46.10, 42.14, 38.49, 26.75, 25.28; ESI–MS m/z = 459.4 $[M + 1]^+$; Anal. Calcd. for $C_{27}H_{27}ClN_4O$: C, 70.65; H, 5.93; N, 12.21, found: C, 70.58; H, 5.75; N, 12.38.

General procedure for the synthesis of *N*-protected anthranilamides 2–9

A solution of the *N*-protected anthranilic acid or halogenoanthranilic acid (0.297 mmol), 0.068 g (0.54 mmol) DIEA and 0.103 g (0.27 mmol) HATU in DMF (1 mL) was stirred at room temperature. After 10 min, 0.27 mmol amino reagent was added to the mixture (0.060 g CQ, 0.096 g PQ or 0.057 g HA). The reaction mixture was stirred overnight at room temperature, diluted with EtOAc, extracted with a 5% solution of NaOH in water (3 × 30 mL) and washed with water (1 × 30 mL). The organic layer was dried through a phase separator, filtrated and evaporated under reduced pressure.

tert-Butyl {5-chloro-2-[[4-[(7-chloroquinolin-4-yl)amino]butyl]carbamoyl]phenyl}carbamate (2) **2** was obtained from the reaction of *N*-Boc-4-chloroanthranilic acid (0.081 g) and after crystallization from acetone as a white solid (0.101 g, 74%); mp 158–160 °C; IR (KBr) (ν_{max}/cm^{-1}): 3333, 3194, 2975, 2938, 2854, 1726, 1629, 1578, 1537, 1506, 1474, 1450, 1430, 1403, 1367, 1325, 1296, 1272, 1246, 1222, 1203, 1153, 1113, 1102, 1081, 1046, 8886, 868, 834, 800, 773, 690, 652, 599, 532, 496; ^{1}H NMR (δ/ppm): 10.67 (s, 1H), 8.87 (t, 1H, J = 5.5 Hz), 8.38 (d, 1H, J = 5.4 Hz), 8.28 (d, 1H, J = 9.1 Hz), 8.22 (d, 1H, J = 9.0 Hz), 7.78 (t, 2H, J = 2.7 Hz), 7.53 (dd, 1H, J = 9.0, 2.5 Hz), 7.44 (dd, 1H, J = 9.0, 2.3 Hz), 7.31 (t, 1H, J = 5.3 Hz), 6.49 (d, 1H, J = 5.5 Hz), 3.33–3.25 (m, 4H), 1.76–1.62 (m, 4H), 1.45 (s, 9H); ^{13}C NMR (δ/ppm): 166.93, 151.97, 151.97, 150.05, 149.10, 138.47, 133.32, 131.67, 127.64, 127.48, 125.17, 124.08, 123.95, 120.92, 120.26, 117.44, 98.64, 80.06, 42.05, 38.89, 27.88, 26.30, 25.24; ESI–MS m/z = 503.4 $[M + 1]^+$; Anal. Calcd. for $C_{25}H_{28}Cl_2N_4O_3$: C, 59.65; H, 5.61; N, 11.13, found: C, 59.79; H, 5.47; N, 10.98.

tert-Butyl {4-bromo-2-[[4-[(7-chloroquinolin-4-yl)amino]butyl]carbamoyl]phenyl}carbamate (3) **3** was obtained from the reaction of *N*-Boc-5-bromoanthranilic acid (0.094 g) and after purification by column chromatography (mobile-phase dichloromethane/methanol 9:1) and crystallization from diethyl ether as a white solid (0.117 g, 79%); mp 184–186 °C; IR (KBr) (ν_{max}/cm^{-1}) 3348, 3261, 2968, 2932,

1723, 1614, 1572, 1542, 1504, 1454, 1432, 1367, 1354, 1325, 1295, 1271, 1246, 1223, 1153, 1083, 1049, 1025, 965, 910, 884, 870, 833, 812, 761, 639, 615, 522, 508; ^{1}H NMR (δ/ppm): 10.68 (s, 1H), 8.88 (t, 1H, J = 5.3 Hz), 8.39 (d, 1H, J = 5.4 Hz), 8.29 (d, 1H, J = 9.1 Hz), 8.17 (d, 1H, J = 9.0 Hz), 7.90 (d, 1H, J = 2.2 Hz), 7.78 (d, 1H, J = 2.1 Hz), 7.65 (dd, 1H, J = 9.0, 2.2 Hz), 7.45 (dd, 1H, J = 9.0, 2.1 Hz), 7.39 (t, 1H, J = 5.0 Hz), 6.50 (d, 1H, J = 5.5 Hz), 3.32 (dd, 4H, J = 11.7, 5.9 Hz), 1.79–1.61 (m, 4H), 1.45 (s, 9H); ^{13}C NMR (δ/ppm): 166.86, 151.93, 151.54, 150.24, 148.70, 138.88, 134.56, 133.49, 130.42, 127.17, 124.14, 121.25, 120.56, 117.37, 113.00, 98.64, 80.08, 42.08, 38.89, 27.87, 26.29, 25.24; ESI–MS m/z = 549.3 $[M+3]^{+}$; Anal. Calcd. for $C_{25}H_{28}BrClN_4O_3$: C, 54.81; H, 5.15; N, 10.23, found: C, 54.85; H, 5.25; N, 10.11.

2-(Benzylamino)-N-{4-[(6-methoxyquinolin-8-yl)amino] pentyl}benzamide (4) **4** was obtained from the reaction of *N*-benzylanthranilic acid (0.067 g) and after purification by column chromatography (mobile-phase cyclohexane/ethyl acetate 1:1) as a brown oil (0.126 g, 80%); IR (film) (ν_{max}/cm^{-1}) 3352, 3061, 3029, 3002, 2960, 2933, 2862, 1710, 1630, 1615, 1594, 1514, 1451, 1422, 1386, 1362, 1334, 1273, 1219, 1200, 11,578, 1051, 1029, 900, 791, 747, 698, 679, 624, 529; ^{1}H NMR (δ/ppm): 8.53 (dd, 1H, J = 4.2, 1.6 Hz), 8.35 (t, 1H, J = 5.5 Hz), 8.20 (t, 1H, J = 5.8 Hz), 8.07 (dd, 1H, J = 8.3, 1.6), 7.52 (dd, 1H, J = 7.9, 1.4 Hz), 7.42 (dd, 1H, J = 8.2, 4.2 Hz), 7.36–7.28 (m, 4H), 7.26–7.20 (m, 1H,), 7.19–7.15 (m, 1H), 6.60 (d, 1H, J = 7.9 Hz), 6.56–6.51 (m, 1H), 6.47 (d, 1H, J = 2.5 Hz), 6.28 (d, 1H, J = 2.5 Hz), 6.15 (d, 1H, J = 8.8 Hz), 4.35 (d, 2H, J = 5.8 Hz), 3.81 (s, 3H), 3.70–3.62 (m, 1H), 3.29–3.20 (m, 2H), 1.77–1.53 (m, 4H), 1.22 (d, 3H, J = 6.3 Hz); ^{13}C NMR (δ/ppm): 169.03, 159.00, 148.89, 144.64, 144.64, 139.60, 134.79, 134.53, 132.01, 129.58, 128.43, 128.23, 127.09, 126.80, 122.09, 115.56, 114.38, 111.41, 96.11, 91.60, 54.97, 47.04, 46.07, 38.82, 33.50, 25.94, 20.20; ESI–MS m/z = 491.5 $[M+23]^{+}$; Anal. Calcd. for $C_{29}H_{32}N_4O_2$: C, 74.33; H, 6.88; N, 11.96, found: C, 74.66; H, 6.79; N, 12.04.

tert-Butyl {5-chloro-2-[[4-[(6-methoxyquinolin-8-yl) amino]pentyl]carbamoyl]phenyl}carbamate (5) **5** was obtained from the reaction of *N*-Boc-4-chloroanthranilic acid (0.081 g) and after purification by column chromatography (mobile-phase cyclohexane/ethyl acetate/methanol 3:1:0.5) as a yellow solid (0.107 g, 77%); mp 66–67 °C; IR (KBr) (ν_{max}/cm^{-1}) 3339, 2973, 2932, 2866, 1726, 1616, 1511, 1454, 1388, 1367, 1246, 1221, 1155, 1050, 1024, 902, 821, 790; ^{1}H NMR (δ/ppm): 10.64 (s, 1H), 8.84 (t, 1H, J = 5.4 Hz), 8.53 (dd, 1H, J = 4.2, 1.6 Hz), 8.21 (d, 1H, J = 9.0 Hz), 8.07 (dd, 1H, J = 8.3, 1.6 Hz), 7.76 (d, 1H, J = 2.5 Hz), 7.52 (dd, 1H, J = 9.0, 2.5 Hz), 7.42 (dd, 1H, J = 8.2, 4.2 Hz), 6.46 (d, 1H, J = 2.5 Hz), 6.27 (d, 1H, J = 2.5 Hz), 6.16 (d, 1H, J = 8.8 Hz), 3.80 (d, 3H, J = 6.5 Hz), 3.70–3.63 (m, 1H), 3.28 (dd, 2H, J = 11.5, 5.6 Hz), 1.76–1.57 (m, 4H), 1.45 (s, 9H), 1.23 (d, 3H, J = 6.3 Hz); ^{13}C NMR (δ/ppm): 166.87, 158.98, 151.97, 145.54, 144.62, 138.43, 134.78, 134.54, 131.60, 129.57, 127.64, 125.16, 122.07, 120.99, 120.22, 96.12, 91.60, 80.02, 54.94, 46.99, 38.88, 33.40, 27.88, 25.49, 20.19; ESI–MS m/z = 513.4 $[M+1]^{+}$; Anal. Calcd. for $C_{27}H_{33}ClN_4O_4$: C, 63.21; H, 6.48; N, 10.92, found: C, 62.70; H, 6.43; N, 11.09.

tert-Butyl {4-bromo-2-[[4-[(6-methoxyquinolin-8-yl) amino]pentyl]carbamoyl]phenyl}carbamate (6) **6** was obtained from the reaction of *N*-Boc-5-bromoanthranilic acid (0.094 g) and after purification by column chromatography (mobile-phase dichloromethane/methanol 9.5:0.5) and crystallization from ether as a yellow solid (0.081 g, 54%); mp 90–92 °C; IR (KBr) (ν_{max}/cm^{-1}) 3326, 2966, 2930, 2867, 1726, 1615, 1578, 1506, 1453, 1388, 1367, 1296, 1246, 1220, 1153, 1049, 1023, 901, 820, 790, 638; ^{1}H NMR (δ/ppm): 10.65 (s, 1H), 8.85 (t, 1H, J = 5.2 Hz), 8.53 (dd, 1H, J = 4.0, 1.1 Hz), 8.16 (d, 1H, J = 9.0 Hz, 1H), 8.07 (d, 1H, J = 8.2 Hz), 7.88 (d, 1H, J = 2.1 Hz), 7.64 (dd, 1H, J = 9.0, 2.0 Hz), 7.42 (dd, 1H, J = 8.2, 4.2 Hz), 6.47 (d, 1H, J = 2.2 Hz), 6.27 (d, 1H, J = 2.1 Hz), 6.16 (d, 1H, J = 8.7 Hz), 3.81 (s, 17), 3.72–3.60 (m, 1H), 3.27 (d, 2H, J = 5.7 Hz), 1.77–1.56 (m, 4H), 1.45 (s, 9H), 1.23 (d, 3H, J = 6.2 Hz); ^{13}C NMR (δ/ppm): 166.79, 158.98, 151.93, 144.62, 144.20, 138.84, 134.78, 134.54, 134.49, 130.46, 129.57, 122.07, 121.32, 120.52, 112.99, 96.12, 91.61, 80.04, 54.95, 46.99, 38.88, 33.38, 27.87, 25.50, 20.19; ESI–MS m/z = 559.4 $[M+3]^{+}$; Anal. Calcd. for $C_{27}H_{33}BrN_4O_4$: C, 58.17; H, 5.97; N, 10.05, found: C, 58.45; H, 5.90; N, 10.33.

2-(Benzylamino)-N-[(1-methyl-9H-pyrido[3,4-b] indol-3-yl)methyl]benzamide (7) **7** was obtained from the reaction of *N*-benzylanthranilic acid (0.067 g,) and after purification by column chromatography (mobile-phase dichloromethane/methanol 8:1) and crystallization from cyclohexane/diethyl ether/petroleum ether as a white solid (0.061 g, 54%); mp 114–116 °C; IR (KBr) (ν_{max}/cm^{-1}) 3633, 3252, 3060, 3028, 2924, 2849, 1625, 1573, 1514, 1450, 1326, 1275, 1250, 1163, 746, 699; ^{1}H NMR (δ/ppm): 11.49 (s, 1H), 8.98 (t, 1H, J = 5.9 Hz), 8.30 (t, 1H, J = 5.8 Hz), 8.15 (d, 1H, J = 7.9 Hz), 7.85 (s, 1H), 7.75 (dd, 1H, J = 7.9, 1.6 Hz), 7.57 (d, 1H, J = 8.1 Hz), 7.54–7.49 (m, 1H), 7.37–7.33 (m, 2H), 7.31 (t, J = 7.6 Hz, 2H), 7.26–7.21 (m, 2H), 7.21–7.17 (m, 1H), 6.65 (dd, 1H, J = 8.5, 1.1 Hz), 6.63–6.57 (m, 1H), 4.66 (d, 2H, J = 5.9 Hz), 4.38 (d, 2H, J = 5.8 Hz), 2.76 (s, 3H); ^{13}C NMR (δ/ppm): 169.17, 149.09, 146.66, 141.12, 140.75, 139.61, 133.50, 132.25, 128.50, 128.45, 127.79, 127.74, 127.11, 126.82, 121.64, 120.99, 119.07, 115.31, 114.52, 111.90, 111.52, 109.42, 46.09, 44.58, 20.33; ESI–MS m/z = 421.2 $[M+1]^{+}$; Anal. Calcd. for $C_{27}H_{24}N_4O$:

C, 77.12; H, 5.75; N, 13.32, found: C, 76.96; H, 5.73; N, 13.67.

tert-Butyl {5-chloro-2-[[(1-methyl-9H-pyrido[3,4-b]indol-3-yl)methyl]carbamoyl]phenyl}carbamate (8) **8** was obtained from the reaction of *N*-Boc-4-chloroanthranilic acid (0.081 g) and after purification by column chromatography (mobile-phase dichloromethane/methanol 9.5:0.5) and crystallization from cyclohexane as a white solid (0.049 g, 40%); mp 203–205 °C; IR (KBr) (ν_{max}/cm^{-1}) 3334, 3185, 3117, 3071, 2987, 2932, 2862, 1634, 1651, 1626, 1597, 1578, 1512, 1440, 1398, 1365, 1355, 1314, 1244, 1159, 1114, 1066, 1050, 1029, 967, 914, 844, 770, 751, 740, 653, 590, 530; ^{1}H NMR (δ/ppm): 11.52 (s, 1H), 10.73 (s, 1H, 9.49 (t, 1H, J = 5.5 Hz), 8.26 (d, 1H, J = 9.0 Hz), 8.20 (d, 1H, J = 7.8 Hz), 7.98 (d, 1H, J = 2.3 Hz), 7.91 (s, 1H), 7.60–7.48 (m, 3H), 7.20 (t, 1H, J = 7.4 Hz), 4.68 (d, 2H, J = 5.6 Hz), 2.77 (s, 3H), 1.44 (s, 9H); ^{13}C NMR (δ/ppm): 167.05, 152.02, 145.60, 141.29, 140.75, 138.64, 133.60, 131.79, 127.98, 127.82, 127.75, 125.28, 121.79, 121.01, 120.88, 120.29, 119.08, 111.90, 109.93, 80.09, 45.01, 27.86, 20.33; ESI–MS m/z = 465.1 $[M+1]^+$; Anal. Calcd. for $C_{25}H_{25}ClN_4O_3$: C, 64.58; H, 5.42; N, 12.05, found: C, 64.27; H, 5.19; N, 12.21.

tert-Butyl {4-bromo-2-[[(1-methyl-9H-pyrido[3,4-b]indol-3-yl)methyl]carbamoyl]phenyl}carbamate (9) **9** was obtained from the reaction of *N*-Boc-5-bromoanthranilic acid (0.094 g) and after purification by column chromatography (mobile-phase dichloromethane/methanol 9.5:0.5) and crystallization from cyclohexane/diethyl ether/petroleum ether as a white solid (0.080 g, (58%); mp 134–136 °C; IR (KBr) (ν_{max}/cm^{-1}) 3339, 2978, 2926, 2850, 1726, 1696, 1627, 1572, 1505, 1437, 1392, 1367, 1314, 1246, 1154, 1099, 1049, 1024, 904, 828, 756, 736; ^{1}H NMR (δ/ppm): 11.52 (s, 1H), 10.74 (s, 1H), 9.50 (s, 1H), 8.20 (d, 2H, J = 8.8 Hz), 8.09 (d, 1H, J = 2.2 Hz), 7.91 (s, 1H), 7.68 (dd, 1H, J = 9.0, 2.2 Hz), 7.58 (d, 1H, J = 8.2 Hz,), 7.53 (d, 1H, J = 7.6 Hz), 7.21 (d, 1H, J = 7.5 Hz), 4.67 (d, 2H, J = 5.6 Hz), 2.77 (s, 3H), 1.44 (s, 9H); ^{13}C NMR (δ/ppm): 166.97, 151.98, 145.60, 141.30, 140.75, 139.06, 134.67, 133.60, 130.75, 127.83, 127.75, 121.79, 121.19, 121.00, 120.59, 119.08, 113.09, 111.90, 109.97, 80.12, 45.01, 27.86, 20.33; ESI–MS m/z = 511.1 $[M+3]^+$; Anal. Calcd. for $C_{25}H_{25}BrN_4O_3$: C, 58.95; H, 4.95; N, 11.00, found: C, 59.15; H, 4.74; N, 11.29.

General procedure for the synthesis of anthranilamides 10–19

Method A: To a solution of 0.1 mmol of *N*-Boc protected compound in MeOH (3 mL), 1 mmol of HCl in MeOH was added dropwise to the flask. The reaction mixture was stirred for 6–24 h at 60 °C. The solvent was removed under reduced pressure.

Method B: To a suspension of *N*-benzyl-protected compound (0.1 mmol) and 10% Pd/C (10 mg) in methanol (3 mL), ammonium formate (0.5 mmol) was added. The reaction mixture was stirred at 65 °C for 0.5–5 h under an inert atmosphere. The catalyst was filtered off, and the mother liquor was concentrated under reduced pressure.

Method C: A suspension of *N*-benzylanthranilic acid (0.067 g,) benzyl-protected compound (0.1 mmol) and 10% Pd/C (10 mg) in methanol (3 mL) was stirred at room temperature for 1–18 h under a hydrogen atmosphere. The catalyst was filtered off, and the mother liquor was concentrated under reduced pressure.

2-(Benzylamino)-N-[4-(quinolin-4-ylamino)butyl]benzamide (10) **10** was obtained by method B (0.5 h, 65 °C), from the reaction of 0.046 g (0.1 mmol) **1** and after purification by column chromatography (mobile-phase dichloromethane/methanol 8.5:1.5) and crystallization from diethyl ether as a white solid (0.026 g; 64%); mp 117–119 °C; IR(ATR) (ν_{max}/cm^{-1}) 3396, 3296, 3252, 3074, 2932, 2849, 2806, 2723, 1751, 1623, 1594, 1575, 1548, 1512, 1449, 1358, 1335, 1278, 12,278, 1152, 1029, 963, 806, 766, 693, 662, 528; ^{1}H NMR (δ/ppm): 8.67 (s, 1H), 8.49 (d, 1H, J = 7.3 Hz), 8.44 (d, 1H, J = 6.4 Hz), 8.42 (t, 1H, J = 5.7 Hz, 8.24 (t, 1H, J = 5.8 Hz), 7.91 (dd, 1H, J = 8.5, 1.3 Hz), 7.84–7.80 (m, 1H), 7.61–7.54 (m, 2H), 7.37–7.28 (m, 4H), 7.26–7.17 (m, 2H), 6.73 (d, 1H, J = 6.5 Hz), 6.62 (d, 1H, J = 7.5 Hz), 6.57–6.52 (m, 1H), 4.35 (d, 2H, J = 5.7 Hz), 3.49 (q, 2H, J = 6.8 Hz), 3.30 (q, 2H, J = 6.5 Hz), 1.78–1.71 (m, 2H), 1.69–1.62 (m, 2H); ^{13}C NMR (δ/ppm): 169.13, 153.53, 148.95, 145.00, 141.32, 139.57, 132.11, 131.73, 128.46, 128.27, 127.11, 126.83, 125.47, 123.10, 122.79, 117.40, 115.39, 114.40, 111.46, 98.02, 46.10, 42.54, 38.41, 26.60, 25.22; ESI–MS m/z = 425.3 $[M+1]^+$; Anal. Calcd. for $C_{27}H_{28}N_4O$: C, 76.39; H, 6.65; N, 13.20, found: C, 76.54; H, 6.78; N, 13.08.

2-Amino-N-[4-(quinolin-4-ylamino)butyl]benzamide (11) **11** was obtained by method C (5 h, r.t.), from the reaction of 0.046 g (0.1 mmol) **1** and after crystallization from diethyl ether/petroleum ether, as a white solid (0.025 g, 60%); mp 66–68 °C; IR(ATR) (ν_{max}/cm^{-1}) 3332, 3064, 2930, 2863, 1627, 1575, 1532, 1519, 1459, 1452, 1436, 1393, 1373, 1229, 1268, 1253, 1160, 1134, 1130, 1035, 844, 809, 748, 701, 656; ^{1}H NMR (δ/ppm): 9.50 (t, 1H, J = 5.3 Hz), 8.67 (d, 1H, J = 8.4 Hz), 8.49 (d, 1H, J = 7.0 Hz), 8.29 (t, 1H, J = 5.5 Hz), 8.01 (d, 1H, J = 8.1 Hz), 7.93 (t, 1H, J = 7.5 Hz), 7.68 (t, 1H, J = 7.4 Hz), 7.48 (dd, 1H, J = 7.9, 1.0 Hz), 7.16 – 7.08 (m, 1H), 6.88 (d, 1H, J = 7.1 Hz), 6.69 (d, 1H, J = 7.7 Hz), 6.49 (t, 1H, J = 7.1 Hz), 6.39 (s, 2H), 3.58 (dd, 2H, J = 12.7, 6.5 Hz), 3.29 (dd, 2H, J = 12.4,

6.4 Hz), 1.81–1.70 (m, 2H), 1.69–1.59 (m, 2H); ^{13}C NMR (δ/ppm): 168.87, 155.35, 149.56, 142.09, 137.81, 133.25, 131.51, 128.02, 126.35, 123.41, 120.10, 116.67, 116.67, 114.84, 114.49, 97.94, 42.72, 38.20, 26.55, 25.11; ESI–MS m/z = 335.4 $[M+1]^+$; Anal. Calcd. for $C_{20}H_{22}N_4O$: C, 71.83; H, 6.63; N, 16.75, found: C, 71.75; H, 6.69; N, 16.70.

2-Amino-4-chloro-N-{4-[(7-chloroquinolin-4-yl)amino] butyl}benzamide (12) **12** was obtained by method A (16 h, 60 °C), from the reaction of 0.050 g (0.1 mmol) **2** as a white solid (0.036 g, 89%); mp 264–266 °C; IR(ATR) (ν_{max}/cm^{-1}) 3235, 3087, 3042, 3037, 2945, 2920, 2858, 2830, 2818, 2802, 2695, 2642, 2623, 2520, 1994, 1923, 1636, 1632, 1592, 1565, 1550, 1485, 1454, 1432, 1385, 1355, 1332, 1322, 1302, 1281, 1231, 1211, 1169, 1151, 1106, 1030, 961, 913, 890, 874, 840, 791, 779, 763, 701, 677, 656; ^{1}H NMR (δ/ppm): 9.75 (t, 1H, J = 5.5 Hz), 8.77 (d, 1H, J = 9.2 Hz), 8.61 (t, 1H, J = 5.2 Hz), 8.51 (d, 1H, J = 7.0 Hz), 8.12 (d, 1H, J = 2.1 Hz), 7.74 (dd, 1H, J = 9.1, 2.1 Hz), 7.64 (d, 1H, J = 2.4 Hz), 7.29 (dd, 1H, J = 8.7, 2.4 Hz), 6.92 (dd, 2H, J = 17.2, 8.0 Hz), 6.42 (s, 2H), 3.57 (q, 2H, J = 6.6 Hz), 3.29 (q, 2H, J = 6.3 Hz), 1.80–1.61 (m, 4H); ^{13}C NMR (δ/ppm): 167.03, 155.30, 145.58, 142.55, 138.55, 137.83, 134.12, 130.32, 126.67, 125.99, 121.26, 119.95, 118.94, 115.46, 98.52, 42.83, 38.41, 26.30, 25.03; ESI–MS m/z = 403.3 $[M+1]^+$; Anal. Calcd. for $C_{20}H_{20}Cl_2N_4O$: C, 59.56; H, 5.00; N, 13.89, found: C, 59.39; H, 4.85; N, 13.97.

2-Amino-5-bromo-N-{4-[(7-chloroquinolin-4-yl)amino] butyl}benzamide (13) **13** was obtained by method A (22 h, 60 °C), from the reaction of 0.055 g (0.1 mmol) **3** as a white solid (0.043 g, 95%); mp 255–257 °C; IR(ATR) (ν_{max}/cm^{-1}) 3243, 3085, 3058, 3032, 2918, 2858, 2822, 2801, 2691, 2639, 2619, 2516, 1995, 1986, 1632, 1616, 1592, 1563, 1547, 1483, 1453, 1433, 1386, 1355, 1333, 1322, 1309, 1230, 1211, 1169, 1152, 1139, 1102, 1096, 1028, 958, 915, 874, 871, 837, 794, 765, 762, 676, 656; ^{1}H NMR (δ/ppm): 9.72 (t, 1H, J = 5.5 Hz), 8.76 (d, 1H, J = 9.2 Hz), 8.59–8.46 (m, 2H), 8.12 (d, 1H, J = 2.1 Hz), 7.74 (dd, 1H, J = 9.1, 2.1 Hz), 7.71 (d, 1H, J = 2.3 Hz), 7.36 (dd, 1H, J = 8.7, 2.3 Hz), 7.00 (s, 2H), 6.89 (d, 1H, J = 7.2 Hz), 6.83 (d, 1H, J = 8.7 Hz), 3.57 (q, 2H, J = 12.7, 6.6 Hz), 3.29 (q, 2H, J = 6.3 Hz), 1.83–1.58 (m, 4H); ^{13}C NMR (δ/ppm): 167.03, 155.30, 145.58, 142.55, 138.55, 137.83, 134.12, 130.32, 126.67, 125.99, 120.63, 119.95, 118.94, 118.61, 115.45, 98.52, 42.83, 38.41, 26.30, 25.03; ESI–MS m/z = 449.2 $[M+3]^+$; Anal. Calcd. for $C_{20}H_{20}BrClN_4O$: C, 53.65; H, 4.50; N, 12.51, found: C, 53.84; H, 4.81; N, 12.68.

2-Amino-N-{4-[(6-methoxyquinolin-8-yl)amino]pentyl} benzamide (14) **14** was obtained by method C (18 h, r.t.), from the reaction of 0.047 g (0.1 mmol) **4** and after purification by column chromatography (mobile-phase cyclohexane/ethyl acetate/methanol 1:1:0.5) and crystallization from ether/petroleum ether as a yellow solid (0.016 g, 41%); mp 123–124 °C; IR(ATR) (ν_{max}/cm^{-1}) 3436, 3400, 3289, 3070, 3009, 2975, 2939, 2857, 1651, 1615, 1592, 1549, 1520, 1452, 1424, 1386, 1319, 1302, 1266, 1225, 1203, 1157, 1056, 1029, 903, 832, 818, 789, 738. 681, 627, 543; ^{1}H NMR (δ/ppm): 8.53 (dd, 1H, J = 4.2, 1.6 Hz), 8.20 (t, 1H, J = 5.5 Hz), 8.07 (dd, 1H, J = 8.3, 1.6 Hz), 7.49–7.38 (m, 2H), 7.16–7.06 (m, 1H), 6.67 (d, 1H, J = 7.5 Hz), 6.52–6.45 (m, 2H), 6.35 (s, 2H), 6.28 (d, 1H, J = 2.4 Hz), 6.15 (d, 1H, J = 8.7 Hz), 3.82 (s, 3H), 3.71–3.60 (m, 1H), 3.27–3.19 (m, 2H), 1.78–1.53 (m, 4H), 1.22 (d, 3H, J = 6.3 Hz); ^{13}C NMR (δ/ppm): 168.76, 159.00, 149.50, 144.64, 144.23, 134.79, 134.53, 131.44, 129.58, 128.98, 122.09, 116.23, 115.01, 114.49, 96.11, 91.60, 54.97, 47.03, 38.75, 33.51, 25.99, 20.20; ESI–MS m/z = 379.2 $[M+1]^+$; Anal. Calcd. for $C_{22}H_{26}N_4O_2$: C, 69.82; H, 6.92; N, 14.80, found: C, 69.99; H, 6.86; N, 15.15.

2-Amino-4-chloro-N-{4-[(6-methoxyquinolin-8-yl) amino]pentyl}benzamide (15) **15** was obtained by method A (6 h, 60 °C), from the reaction of 0.051 g (0.1 mmol) **5** as an orange solid (0.037 g, 90%); mp 220–222 °C; IR(ATR) (ν_{max}/cm^{-1}) 3311, 3221, 3161, 3111, 3030, 3010, 2975, 2957, 2930, 2861, 2805, 2707, 2586, 1969, 1879, 1639, 1611, 1586, 1534, 1474, 1456, 1424, 1387, 1364, 1324, 1319, 1199, 1167, 1233, 1130, 1033, 898, 841, 811, 762, 672, 617, 542, 503; ^{1}H NMR (δ/ppm): δ 8.75 (d, 1H, J = 4.1 Hz), 8.66 (d, 1H, J = 7.8 Hz), 8.56 (t, 1H, J = 5.1 Hz), 7.85–7.75 (m, 1H), 7.63 (d, 1H, J = 2.0 Hz), 7.31 (dd, 1H, J = 8.6, 1.8 Hz), 6.97 (d, 1H, J = 8.6 Hz), 6.86 (s, 1H), 6.64 (s, 1H), 3.88 (s, 3H), 3.82–3.72 (m, 1H), 3.25 (d, 2H, J = 5.1 Hz), 1.86–1.58 (m, 4H), 1.27 (d, 3H, J = 6.2 Hz); ^{13}C NMR (δ/ppm): 166.67, 160.09, 148.50, 143.24, 141.92, 140.76, 131.35, 131.26, 127.65, 122.18, 121.92, 120.47, 119.55, 101.14, 94.01, 55.53, 48.37, 32.69, 25.49, 19.57; ESI–MS m/z = 413.3 $[M+1]^+$; Anal. Calcd. for $C_{22}H_{25}ClN_4O_2$: C, 63.99; H, 6.10; N, 13.57, found: C, 63.86; H, 5.99; N, 13.67.

2-Amino-5-bromo-N-{4-[(6-methoxyquinolin-8-yl) amino]pentyl}benzamide (16) **16** was obtained by method A (19 h, 60 °C), from the reaction of 0.058 g (0.1 mmol) **6** as an orange solid (0.034 g, 74%); mp 141–142 °C; IR(ATR) (ν_{max}/cm^{-1}) 3331, 3227, 3090, 3069, 3025, 2967, 2938, 2866, 2735, 2655, 2615, 2544, 2462, 1998, 1899, 1815, 1637, 1608, 1591, 1538, 1466, 1389, 1356, 1334, 1305, 1278, 1238, 1221, 1202, 1178, 1168, 1147, 1131, 1059, 1028, 1006, 902, 833, 820, 777, 761, 678, 659, 624, 517; ^{1}H NMR (δ/ppm): 8.75 (dd, 1H, J = 4.9, 1.5 Hz), 8.64 (d, 2H, J = 8.3 Hz), 8.52 (t, 1H, J = 5.2 Hz), 7.78 (dd, 1H, J = 8.4, 4.9 Hz), 7.71 (d, 1H, J = 2.3 Hz), 7.38 (dd, 1H, J = 8.7, 2.3 Hz), 6.86 (d, 2H, J = 8.8 Hz), 6.63 (s, 1H),

3.88 (s, 3H), 3.77 (dd, 1H, $J = 12.2$, 6.1 Hz), 3.24 (q, 2H, $J = 6.2$ Hz), 1.84–1.58 (m, 4H), 1.26 (d, 3H, $J = 6.3$ Hz); ^{13}C NMR (δ/ppm): 166.79, 160.07, 144.73, 141.62, 141.00, 140.33, 138.34, 134.12, 131.23, 131.23, 122.19, 120.34, 119.29, 108.55, 93.96, 55.52, 48.37, 38.90, 32.75, 25.55, 19.61; ESI–MS $m/z = 457.3$ $[M + 1]^+$; Anal. Calcd. for $C_{22}H_{25}BrN_4O_2$: C, 57.77; H, 5.51; N, 12.25, found: C, 57.97; H, 5.79; N, 12.51.

2-Amino-N-[(1-methyl-9H-pyrido[3,4-b]indol-3-yl) methyl]benzamide (17) **17** was obtained by method B (1 h, 65 °C), from the reaction of 0.042 g (0.1 mmol) **7** and after crystallization from diethyl ether as an off-white solid (0.022 g, 73%); mp 127–130 °C; IR(ATR) (ν_{max}/cm^{-1}) 3435, 3330, 3149, 3109, 3057, 2946, 2926, 2878, 2794, 2711, 1633, 1574, 1524, 1451, 1355, 1341, 1289, 1248, 1161, 1151, 1150, 1133, 1107, 1032, 962, 906, 840, 774, 751, 729, 529; ^{1}H NMR (δ/ppm): 11.51 (s, 1H), 8.82 (t, 1H, $J = 5.9$ Hz), 8.21–8.13 (m, 2H), 7.84 (s, 1H), 7.66 (d, 1H, $J = 7.6$ Hz), 7.57 (d, 1H, $J = 8.2$ Hz), 7.51 (t, 1H, $J = 7.6$ Hz), 7.19 (t, 1H, $J = 7.5$ Hz), 7.16 (t, 1H, $J = 7.6$ Hz), 6.72 (d, 1H, $J = 8.2$ Hz), 6.45 (s, 2H), 4.65 (d, 2H, $J = 5.8$ Hz), 2.77 (s, 3H); ^{13}C NMR (δ/ppm): 168.86, 149.71, 146.78, 141.09, 140.76, 133.49, 131.67, 128.21, 127.78, 127.74, 121.65, 120.99, 119.08, 116.35, 114.79, 114.65, 111.90, 109.43, 44.48, 20.32; ESI–MS $m/z = 331.2$ $[M + 1]^+$; Anal. Calcd. for $C_{20}H_{18}N_4O$: C, 72.71; H, 5.49; N, 16.96, found: C, 72.84; H, 5.71; N, 16.78.

2-Amino-4-chloro-N-[(1-methyl-9H-pyrido[3,4-b] indol-3-yl)methyl]benzamide (18) **18** was obtained by method A (24 h, 60 °C), from the reaction of 0.046 g (0.1 mmol) **8** as a white solid (0.028 g, 77%); mp 206–209 °C; IR(ATR) (ν_{max}/cm^{-1}) 3395, 3118, 3018, 2939, 2934, 2870, 2607, 2571, 1655, 1640, 1560, 1509, 1461, 1368, 1343, 1315, 1248, 1135, 1103, 985, 888, 863, 825, 752, 71; ^{1}H NMR (δ/ppm): 13.04 (s, 1H), 9.33 (t, 1H, $J = 5.6$ Hz), 8.53 (s, 1H), 8.50 (d, 1H, $J = 8.1$ Hz), 7.84 (d, 1H, $J = 2.5$ Hz), 7.78–7.73 (m, 2H), 7.43–7.37 (m, 1H), 7.27 (dd, 1H, $J = 8.8$, 2.5 Hz), 6.86 (d, 1H, $J = 8.8$ Hz), 4.90 (d, 2H, $J = 5.5$ Hz), 4.77 (s, 2H), 3.13 (s, 3H); ^{13}C NMR (δ/ppm): 167.73, 143.67, 140.19, 138.45, 133.12, 132.20, 132.03, 131.38, 127.86, 123.63, 121.17, 119.70, 119.17, 113.49, 112.78, 40.13, 15.84; ESI–MS $m/z = 365.1$ $[M + 1]^+$; Anal. Calcd. for $C_{20}H_{17}ClN_4O$: C, 65.84; H, 4.70; N, 15.36, found: C, 65.99; H, 4.86; N, 15.35.

2-Amino-5-bromo-N-[(1-methyl-9H-pyrido[3,4-b] indol-3-yl)methyl]benzamide (19) **19** was obtained by method A (24 h, 60 °C), from the reaction of 0.051 g (0.1 mmol) **9** as a white solid; mp 242–244 °C (decomp.) (0.037 g, 90%); IR(ATR) (ν_{max}/cm^{-1}) 3377, 3268, 3013, 2867, 2607, 2568, 1923, 1747, 1640, 1574, 1506, 1489, 1430, 1392, 1377, 1342, 1328, 1287, 1253, 1168, 1146, 1100, 988, 909, 881, 838, 826, 752, 712, 542, 502; ^{1}H NMR (δ/ppm): 13.05 (s, 1H), 9.32 (t, 1H, $J = 5.6$ Hz), 8.53 (s, 1H), 8.49 (d, 1H, $J = 8.1$ Hz), 7.94 (d, 1H, $J = 2.3$ Hz), 7.79–7.73 (m, 2H), 7.42–7.35 (m, 2H), 6.80 (d, 1H, $J = 8.8$ Hz), 4.92–4.88 (m, 2H), 4.78 (s, 2H), 3.13 (s, 3H); ^{13}C NMR (δ/ppm): 167.65, 143.67, 140.18, 138.43, 134.74, 133.11, 132.18, 131.37, 130.64, 123.62, 121.15, 119.68, 119.54, 113.49, 112.78, 40.13, 15.84; ESI–MS $m/z = 409.0$ $[M + 1]^+$; Anal. Calcd. for $C_{20}H_{17}BrN_4O$: C, 58.69; H, 4.19; N, 13.69, found: C, 58.99; H, 4.09; N, 13.35.

Antiproliferative activity assays

Adherent cell lines LN-229, Capan-1, HCT-116 and NCI-H460 cells were seeded at a density between 500 and 1500 cells per well, in 384-well tissue culture plates (Greiner). After overnight incubation, cells were treated with the test compounds. After incubation for 3 days at 37 °C, the formazan-based 3-(4,5-dimethylthiazol-2-yl)-5-(3-carboxymethoxyphenyl)-2-(4-sulfophenyl)-2*H*-tetrazolium (MTS) cell viability assay (CellTiter 96® AQueous One Solution Cell Proliferation Assay, Promega) was performed to assess cell viability, and the spectrophotometric data were used to calculate the IC_{50} values [61–65].

Suspension cell lines DND-41, HL-60, K-562 and Z-138 were seeded at densities ranging from 2500 to 5500 cells per well in 384-well tissue culture plates containing the test compounds at the same concentration points. The plates were incubated at 37 °C and monitored for 72 h in an IncuCyte® device (Essen BioScience Inc.) for real-time imaging. Images were taken every 3 h, with one field imaged per well under 10 × magnification. Cell growth was then quantified based on the percent cellular confluence as analyzed by the IncuCyte® image analysis software and used to calculate IC_{50} values by linear interpolation.

Antiviral activity assays

The antiviral evaluation of anthranilamides **1–19** against influenza viruses A/H1N1 A/Ned/378/05, A/H3N2 A/HK/7/87, B/H1N1 and B/Ned/537/05, respiratory syncytial virus and human coronaviruses HCoV-229E and HCoV-OC43 was performed by seeding MDCK, Hep-2 or HEL 299 cells into 384-well dishes. The previously described procedure was applied [66, 67]. Briefly, after 24 h at 37 °C, serial dilutions of the compounds were added to the cells prior to infection. At 4 days post-infection (influenza and RSV) or 7 days post-infection (HCoV), the virus-induced cytopathogenic effect was measured colorimetrically by the formazan-based MTS assay (CellTiter 96® AQueous One Solution Cell Proliferation Assay), and the antiviral activity was expressed as the 50% effective concentration (EC_{50}). In

parallel, the 50% cytotoxic concentration (CC_{50}) was derived from mock-infected MDCK, Hep-2 or HEL 299 cells. The activities were compared with reference compounds such as zanamivir, ribavirin, rimantadine, ribavirin, DS-10.000, and remdesivir, respectively.

The antiretroviral assays in MT-4 cells have previously been described in detail [62]. Briefly, MT-4 cells (1×10^6 cells/mL) were pre-incubated for 30 min at 37 °C with the test compounds in a 96-well plate. Next, HIV-1 NL4.3 or HIV-2 ROD strains were added according to the $CCID_{50}$ of the viral stock. The CPE was scored microscopically 5 days post-infection, and the EC_{50} values were determined using the MTS/PES method [68].

Anti-QS and bactericidal activity screening

The previously reported screening method using *C. violaceum* ATCC31532 (ATCC; Wesel, Germany) as the reporter was applied to test if the anthranilamides show anti-QS/-biofilm or bactericidal activities [54, 59, 69]. Shortly, the *C. violaceum* strain was cultured overnight at 27 °C on Luria-Berthani agar (Fischer Scientific, Leicestershire, UK) LBA to produce single colonies, which were suspended in PDYT (0.5% peptone, 0.3% D-glucose, 0.25% yeast extract, 0.05% L-tryptophan, *m/v*) to achieve OD600 = 0.02. The obtained cell suspension (200 µL at OD600 = 0.02) with 2% DMSO (control) or with the indicated compounds dissolved in DMSO and tested at varying concentrations (400, 200, 100, 40 and 10 µM) were added into the wells in two parallel 96-well plates (Tissue Culture Treated, polystyrene, flat-bottom, Becton Dickinson). In both 96-well plate, quercetin [70] and azithromycin (Sigma-Aldrich) at 400 µM (dissolved in DMSO as 20 mM stocks) were used as positive controls for QS inhibition and cell viability (bactericidal agent), respectively. The plates were incubated at 27 °C under aerobic conditions (200 r.p.m.) for 22 h. Resazurin, a redox-sensitive dye that is reduced to fluorescent resorufin only by viable cells, was added at 200 µM per each well in the first 96-well plate to assess the bactericidal effects of the compounds [71, 72]. The 96-well plates, with/without the resazurin, were shaken for an additional 30 min (200 r.p.m.) in dark and then centrifuged (4000 rpm, for 20 min, 20 °C) to pellet insoluble violacein and cells. Resorufin containing supernatants (100 µL) were transferred into a new plate and the produced/remaining fluorescence was recorded with a PerkinElmer Victor3 multilabel microtiter plate reader using an excitation/emission wavelengths of 550/590 nm. Supernatants from the 96-well plate without the added resazurin were removed and the pelleted violacein was dissolved in 96% (*v/v*) ethanol. The supernatants with soluble violacein were cleared from cells by centrifugation (4000 rpm, for 20 min, 20 °C), the supernatants (100 µL) were transferred into new 96-well plate and changes in violacein yield were monitored at 595 nm using the PerkinElmer Victor3 reader. Both the anti-QS screening and bactericidal experiment was repeated three times with at least three technical replicates in each plate. Statistical parameters (Z´, S/N and S/B) [73, 74] for each assay were calculated throughout the screening process to monitor assay performance and confirm high quality of the obtained results. Potency (half inhibitory concentrations, IC_{50}) calculation was conducted using the GraphPad Prism version 8 (GraphPad software Inc., San Diego, CA, USA).

Supplementary Information The online version contains supplementary material available at https://doi.org/10.1007/s11030-021-10347-8.

Acknowledgements The study was supported by the Croatian Science Foundation through the research project IP-09-2014-1501 and by the Academy of Finland grant (decision no. 322012 and 325784). The work of doctoral student M. Beus has been fully supported by the Young researcher's career development project—training of doctoral students of the Croatian Science Foundation founded by the European Union from the European Social Fund.

References

1. Schütz C, Empting M (2018) Targeting *Pseudomonas* quinolone signal quorum sensing system for the discovery of novel anti-infective pathoblockers. Beilstein J Org Chem 14:2627–2645. https://doi.org/10.3762/bjoc.14.241
2. Lemke TL, Williams DA, Roche VF, Zito SW (2008) Foye's principles of medicinal chemistry, 6th edn. Wolters Kluwer (Health)/Lippincott Williams & Wilkins, Philadelphia
3. Selby TP, Lahm GP, Stevenson TM (2016) A retrospective look at anthranilic diamide insecticides: discovery and lead optimization to chlorantraniliprole and cyantraniliprole. Pest Management Sci 73:68–665. https://doi.org/10.1002/ps.4308
4. Darakhshan S, Pour AB (2015) Tranilast: a review of its therapeutic applications. Pharmacol Res 91:15–28. https://doi.org/10.1016/j.phrs.2014.10.009
5. Chakrabarti R, Subramaniam V, Abdalla S, Jothy S, Prud'homme GJ (2009) Tranilast inhibits the growth and metastasis of mammary carcinoma. Anticancer Drugs 20:334–345. https://doi.org/10.1097/CAD.0b013e328327994e
6. Subramaniam V, Chakrabarti R, Prud'homme GJ, Jothy S (2010) Tranilast inhibits cell proliferation and migration and promotes apoptosis in murine breast cancer. Anticancer Drugs 21:351–361. https://doi.org/10.1097/CAD.0b013e328334992c
7. Raffa D, Maggio B, Plescia F, Cascioferro S, Plescia S, Raimondi MV, Daidone G, Tolomeo M, Grimaud S, Cristina AD, Pipitone RM, Bai R, Hamel E (2011) Synthesis, antiproliferative activity, and mechanism of action of a series of 2-{[(2*E*)-3-phenylprop-2-enoyl]amino}benzamides. Eur J Med Chem 46:2786–2796. https://doi.org/10.1016/j.ejmech.2011.03.067
8. Subramaniam V, Ace O, Prud'homme GJ, Jothy S (2011) Tranilast treatment decreases cell growth, migration and inhibits colony formation of human breast cancer cells. Exp Mol Pathol 90:116–122. https://doi.org/10.1016/j.yexmp.2010.10.012
9. Rogosnitzky M, Danks R, Kardash E (2012) Therapeutic potential of tranilast, an anti-allergy drug, in proliferative disorders. Anticancer Res 32:2471–2478
10. Rojas-Puentes LL, Gonzales-Pinedo M, Crismatt A, Ortega-Gomez A, Gamboa-Vignolle C, Nuñez-Gomez R,

Dorantes-Gallareta Y, Arce-Salinas C, Arrieta O (2013) Phase II randomized, double-blind, placebo-controlled study of whole-brain irradiation with concomitant chloroquine for brain metastases. Radiat Oncol 8:209. https://doi.org/10.1186/1748-717X-8-209
11. Verbaanderd C, Maes H, Schaaf MB, Sukhatme VP, Pantziarka P, Sukhatme V, Agostinis P, Bouche G (2017) Repurposing drugs in oncology (ReDO)—chloroquine and hydroxychloroquine as anti-cancer agents. Cancer 11:781. https://doi.org/10.3332/ecancer.2017.781
12. Wang F, Tang J, Li P, Si S, Yu H, Yang X, Tao J, Lv Q, Gu M, Yang H, Wang Z (2018) Chloroquine enhances the radiosensitivity of bladder cancer cells by inhibiting autophagy and activating apoptosis. Cell Physiol Biochem 45:54–66. https://doi.org/10.1159/000486222
13. ClinicalTrials.gov. https://clinicaltrials.gov/ct2/home. Accessed 30 Mar 2021
14. Das AK (2015) Anticancer effect of antimalarial artemisinin compounds. Ann Med Health Sci Res 5:93–102. https://doi.org/10.4103/2141-9248.153609
15. Wong YK, Xu C, Kalesh KA, He Y, Lin Q, Fred Wong WS, Shen H-M, Wang J (2017) Artemisinin as an anticancer drug: Recent advances in target profiling and mechanisms of action. Med Res Rev 37:1492–1517. https://doi.org/10.1002/med.21446
16. Zhang Y, Xu G, Zhang S, Wang D, Prabha PS, Zuo Z (2018) Antitumor research on artemisinin and its bioactive derivatives. Nat Prod Bioprospect 8:303–319. https://doi.org/10.1007/s13659-018-0162-1
17. Pavić K, Rajić Z, Mlinarić Z, Uzelac L, Kralj M, Zorc B (2018) Chloroquine urea derivatives: synthesis and antitumor activity in vitro. Acta Pharm 68:471–483. https://doi.org/10.2478/acph-2018-0039
18. Zorc B, Perković I, Pavić K, Rajić Z, Beus M (2019) Primaquine derivatives: modifications of the terminal amino group. Eur J Med Chem 182:111640. https://doi.org/10.1016/j.ejmech.2019.111640
19. Sobhani AM, Ebrahimi SA, Mahmoudian M (2002) An in vitro evaluation of human DNA topoisomerase I inhibition by *Peganum harmala* L. seeds extract and its beta-carboline alkaloids. J Pharm Pharm Sci 5:19–23
20. Chen Q, Chao R, Chen H, Hou X, Yan H, Zhou S, Peng W, Xu A (2004) Antitumor and neurotoxic effects of novel harmine derivatives and structure-activity relationship analysis. Int J Cancer 114:675–682
21. Cao R, Chen Q, Hou X, Chen H, Guan H, Ma Y, Peng W, Xu A (2004) Synthesis, acute toxicities, and antitumor effects of novel 9-substituted beta-carboline derivatives. Bioorg Med Chem 12:4613–4623. https://doi.org/10.1016/j.bmc.2004.06.038
22. Cao R, Peng W, Chen H, Ma Y, Liu X, Hou X, Guan H, Xu A (2005) DNA binding properties of 9-substituted harmine derivatives. Biochem Biophys Res Commun 338:1557–1563. https://doi.org/10.1016/j.bbrc.2005.10.121
23. Cao R, Chen H, Peng W, Ma Y, Hou X, Guan H, Liu X, Xu A (2005) Design, synthesis and in vitro and in vivo antitumor activities of novel beta-carboline derivatives. Eur J Med Chem 40:991–1001. https://doi.org/10.1016/j.ejmech.2005.04.008
24. Cao R, Guan X, Shi B, Chen Z, Ren Z, Peng W, Song H (2010) Design, synthesis and 3D-QSAR of β-carboline derivatives as potent antitumor agents. Eur J Med Chem 45:2503–2515. https://doi.org/10.1016/j.ejmech.2010.02.036
25. Egusa H, Doi M, Saeki M, Fukuyasu S, Akashi Y, Yokota Y, Yatani H, Kamisaki Y (2011) The small molecule harmine regulates NFATc1 and Id2 expression in osteoclast progenitor cells. Bone 49:264–274. https://doi.org/10.1016/j.bone.2011.04.003
26. Patel K, Gadewar M, Tripathi R, Prasad SK, Patel DK (2012) A review on medicinal importance, pharmacological activity and bioanalytical aspects of beta-carboline alkaloid "Harmine." Asian Pac J Trop Biomed 2:660–664. https://doi.org/10.1016/S2221-1691(12)60116-6
27. Dai F, Chen Y, Song Y, Huang L, Zhai D, Dong Y, Lai L, Zhang T, Li D, Pang X, Liu M, Yi Z (2012) A natural small molecule harmine inhibits angiogenesis and suppresses tumour growth through activation of p53 in endothelial cells. PLoS ONE 7:e52162. https://doi.org/10.1371/journal.pone.0052162
28. Frédérick R, Bruyère C, Vancraeynest C, Reniers J, Meinguet C, Pochet L, Backlund A, Masereel B, Kiss R, Wouters J (2012) Novel trisubstituted harmine derivatives with original in vitro anticancer activity. J Med Chem 55:6489–6501. https://doi.org/10.1021/jm300542e
29. Cuny GD, Ulyanovac NP, Patnaik D, Liu JF, Lin X, Auerbach K, Ray SS, Xian J, Glicksman MA, Steina RL, Higgins JMB (2012) Structure-activity relationship study of beta-carboline derivatives as haspin kinase inhibitors. Bioorg Med Chem Lett 22:2015–2019. https://doi.org/10.1016/j.bmcl.2012.01.028
30. Hara ES, Ono M, Kubota S, Sonoyama W, Oida Y, Hattori T, Nishida T, Furumatsu T, Ozaki T, Takigawa M, Kuboki T (2013) Novel chondrogenic and chondroprotective effects of the natural compound harmine. Biochimie 95:374–381. https://doi.org/10.1016/j.biochi.2012.10.016
31. Cao R, Fan W, Guo L, Ma Q, Zhang G, Li J, Chen X, Ren Z, Qiu L (2013) Synthesis and structure-activity relationships of harmine derivatives as potential antitumor agents. Eur J Med Chem 60:135–143. https://doi.org/10.1016/j.ejmech.2012.11.045
32. Shi B, Cao R, Fan W, Guo L, Ma Q, Chen X, Zhang G, Qiu L, Song H (2013) Design, synthesis and in vitro and in vivo antitumor activities of novel bivalent β-carbolines. Eur J Med Chem 60:10–20. https://doi.org/10.1016/j.ejmech.2012.11.033
33. Li S, Wang A, Gu F, Wang Z, Tian C, Qian Z, Tang L, Gu X (2015) Novel harmine derivatives for tumor targeted therapy. Oncotarget 6:8988–9001. https://doi.org/10.18632/oncotarget.3276
34. Zhang XF, Sun RQ, Jia YF, Chen Q, Tu RF, Li KK, Zhang XD, Du RL, Cao RH (2016) Synthesis and mechanisms of action of novel harmine derivatives as potential antitumor agents. Sci Rep 6:33204. https://doi.org/10.1038/srep33204
35. Carvalho A, Chu J, Meinguet C, Kiss R, Vandenbussche G, Masereel B, Wouters J, Kornienko A, Pelletier J, Mathieu V (2017) A harmine-derived beta-carboline displays anti-cancer effects in vitro by targeting protein synthesis. Eur J Pharmacol 805:25–35. https://doi.org/10.1016/j.ejphar.2017.03.034
36. Perković I, Raić-Malić S, Fontinha D, Prudêncio M, Pessanha de Carvalho L, Held J, Tandarić T, Vianello R, Zorc B, Rajić Z (2020) Harmicines—harmine and cinnamic acid hybrids as potential antiplasmodial hits. Eur J Med Chem 187:111927. https://doi.org/10.1016/j.ejmech.2019.111927
37. Marinović M, Perković I, Fontinha D, Prudêncio M, Held J, Pessanha de Carvalho L, Tandarić T, Vianello R, Zorc B, Rajić Z (2020) Novel harmicines with improved potency against *Plasmodium*. Molecules 25:4376. https://doi.org/10.3390/molecules25194376
38. Zhao M, Bi L, Wang W, Wang C, Baudy-Floc'h M, Ju J, Peng S (2006) Synthesis and cytotoxic activities of β-carboline amino acid ester conjugates. Bioorg Med Chem 14:6998–7010. https://doi.org/10.1016/j.bmc.2006.06.021
39. Savarino A, Boelaert JR, Cassone A, Majori G, Cauda R (2003) Effects of chloroquine on viral infections: an old drug against today's diseases? Lancet Infect Dis 3:722–727. https://doi.org/10.1016/S1473-3099(03)00806-5
40. Al-Bari MAA (2017) Targeting endosomal acidification by chloroquine analogs as a promising strategy for the treatment of emerging viral diseases. Pharmacol Res Perspect 5:e00293. https://doi.org/10.1002/prp2.293

41. Keyaerts E, Vijgen L, Maes P, Neyts J, Van Ranst M (2004) In vitro inhibition of severe acute respiratory syndrome coronavirus by chloroquine. Biochem Biophys Res Comm 323:264–264. https://doi.org/10.1016/j.bbrc.2004.08.085
42. Colson P, Rolain JM, Raoult D (2020) Chloroquine for the 2019 novel coronavirus SARS Cov2. Int J Antimicrob Agents 55:105923. https://doi.org/10.1016/j.ijantimicag.2020.105923
43. Wang M, Cao R, Zhang L, Yang X, Liu J, Xu M, Shi Z, Hu Z, Zhong W, Xiao G (2020) Remdesivir and chloroquine effectively inhibit the recently emerged novel coronavirus (2019-nCoV) in vitro. Cell Res 30:269–271. https://doi.org/10.1038/s41422-020-0282-0
44. Devaux CA, Rolain JM, Colson P, Raoult D (2020) New insights on the antiviral effects of chloroquine agains coronavirus: what to expect for COVID-19? Int J Antimicrob Agents 55:105938. https://doi.org/10.1016/j.ijantimicag.2020.105938
45. Cortegiani A, Ingoglia G, Ippolito M, Giarratano A, Einav S (2020) A systematic review on the efficacy and safety of chloroquine for the treatment of COVID-19. J Crit Care 57:279–283. https://doi.org/10.1016/j.jcrc.2020.03.005
46. Abu-Dief AM (2020) Chloroquine and hydroxychloroquine in the management of coronavirus: Cares and challenges. Mod Appro Drug Des 3:MADD.000552.20209. https://doi.org/10.31031/MADD.2020.03.000552
47. Gao J, Tian Z, Yang X (2020) Breakthrough: chloroquine phosphate has shown apparent efficacy in treatment of COVID-19 associated pneumonia in clinical studies. BioSci Trends 14:72–73. https://doi.org/10.5582/bst.2020.01047
48. Hudson JB, Graham EA, Towers GH (1986) Antiviral effect of harmine, a photoactive beta-carboline alkaloid. Photochem Photobiol 43:21–26. https://doi.org/10.1111/j.1751-1097.1986.tb05586.x
49. Hudson JB, Graham EA, Fong R, Hudson LL, Towers GH (1986) Further studies on the antiviral activity of harmine, a photoactive beta-carboline alkaloid. Photochem Photobiol 44:483–487. https://doi.org/10.1111/j.1751-1097.1986.tb04696.x
50. Chen D, Su A, Fu Y, Wang X, Lv X, Xu W, Xu S, Wang H, Wu Z (2015) Harmine blocks herpes simplex virus infection through downregulating cellular NF-κB and MAPK pathways induced by oxidative stress. Antiviral Res 123:27–38. https://doi.org/10.1016/j.antiviral.2015.09.003
51. Moradi MT, Karimi A, Fotouhi F, Kheiri S, Tobabi A (2017) In vitro and in vivo effects of *Peganum harmala* L. seeds extract against influenza A virus. Avicenna J Phytomed 7:519–530
52. Jiang X, Zou J, Zhuang Y, Yuan W, Zhu L, Zhu G (2017) The antiviral effects of harmine against BoHV-1 infection in vitro. Lett Drug Design Discov 14:1303. https://doi.org/10.2174/1570180814666170425155554
53. Ilangovan A, Fletcher M, Rampioni G, Pustelny C, Rumbaugh K, Heeb S, Cámara M, Truman A, Ram Chhabra S, Emsley J, Williams P (2013) Structural basis for native agonist and synthetic inhibitor recognition by the *Pseudomonas aeruginosa* quorum sensing regulator PqsR (MvfR). PLoS Pathog 9:e1003508. https://doi.org/10.1371/journal.ppat.1003508
54. Beus M, Savijoki K, Patel JZ, Yli-Kauhaluoma J, Fallarero A, Zorc B (2020) Chloroquine fumardiamides as novel quorum sensing inhibitors. Biorg Med Chem Lett 30:127336. https://doi.org/10.1016/j.bmcl.2020.127336
55. Sung Y, Koike K, Nikaido T, Ohmoto T, Sankawa U (1984) Inhibitors of cyclic AMP phosphodiesterase in *Picrasma quassioides* Bennet, and inhibitory activities of related beta-carboline alkaloids. Chem Pharm Bull (Tokyo) 32:1872–1877. https://doi.org/10.1248/cpb.32.1872
56. Eagon S, Anderson MO (2014) Microwave-assisted synthesis of tetrahydro-β-carbolines and β-carbolines. Eur J Org Chem 8:1653–1665. https://doi.org/10.1002/ejoc.201301580
57. Chemicalize, 2017, ChemAxon Ltd. http://www.chemicalize.org
58. Balzarini J, Holy A, Jindrich J, Naesens L, Snoeck R, Schols D, De Clercq E (1993) Differential antiherpesvirus and antiretrovirus effects of the (*S*) and (*R*) enantiomers of acyclic nucleoside phosphonates: potent and selective in vitro and in vivo antiretrovirus activities of (*R*)-9-(2-phosphonomethoxypropyl)-2,6-diaminopurine. Antimicrob Agents Chemother 37:332–338. https://doi.org/10.1128/AAC.37.2.332
59. McClean KH, Winson MK, Fish L, Taylor A, Chhabra SR, Camara M, Daykin M, Lamb JH, Swift S, Bycroft BW, Stewart GS, Williams P (1997) Quorum sensing and *Chromobacterium violaceum*: exploitation of violacein production and inhibition for the detection of *N*-acylhomoserine lactones. Microbiology 143:3703–3711. https://doi.org/10.1099/00221287-143-12-3703
60. Zhou L, Zhang Y, Ge Y, Zhu X, Pan J (2020) Regulatory mechanisms and promising applications of quorum sensing-inhibiting agents in control of bacterial biofilm formation. Front Microbiol 11:589640. https://doi.org/10.3389/fmicb.2020.589640
61. Aljohani FS, Abu-Dief AM, El-Khatib RM, Al-Abdulkarim HA, El-Metwaly NM (2021) Structural inspection for novel Pd(II), VO(II), Zn(II) and Cr(III)- azomethine metal chelates: DNA interaction, biological screening and theoretical treatments. J Mol Struct 1246:131139. https://doi.org/10.1016/j.molstruc.2021.131139
62. Abu-Dief AM, Abdel-Rahman LH, Abdel-Mawgoud AAH (2020) A robust *in vitro* anticancer, antioxidant and antimicrobial agents based on new metal-azomethine chelates incorporating Ag(I), Pd(II) and VO(II) cations: Probing the aspects of DNA interaction. Appl Organomet Chem 34:e5373. https://doi.org/10.1002/aoc.5373
63. Abu-Dief AM, El-Metwaly NM, Alzahrani SO, Alkhatib F, El-Remaily MAEAAA (2021) Synthesis and characterization of Fe(III), Pd(II) and Cu(II)-thiazole complexes; DFT, pharmacophore modeling, in-vitro assay and DNA binding studies. J Mol Liquids 326:115277. https://doi.org/10.1016/j.molliq.2021.115277
64. Abdel-Rahman LH, Abu-Dief AM, Atlam FM, Abdel-Mawgoud AAH, Alothman AA, Alsalme AM, Nafady A (2020) Chemical, physical, and biological properties of Pd(II), V(IV)O, and Ag(I) complexes of N3 tridentate pyridine-based Schiff base ligand. J Coord Chem 73:3150–3173. https://doi.org/10.1080/00958972.2020.1842378
65. Abu-Dief AM, El-Sagher HM, Shehata MR (2019) Fabrication, spectroscopic characterization, calf thymus DNA binding investigation, antioxidant and anticancer activities of some antibiotic azomethine Cu(II), Pd(II), Zn(II) and Cr(III) complexes. Appl Organomet Chem 33:e4943. https://doi.org/10.1002/aoc.4943
66. Baggen J, Persoons L, Vanstreels E, Jansen S, Van Looveren D, Boeckx B, Geudens V, De Man J, Jochmans D, Wauters J, Wauters E, Vanaudenaerde BM, Lambrechts D, Neyts J, Dallmeier K, Thibaut HJ, Jacquemyn M, Maes P, Daelemans D (2021) Genome-wide CRISPR screening identifies TMEM106B as a proviral host factor for SARS-CoV-2. Nat Genet. https://doi.org/10.1038/s41588-021-00805-2 (Advance online publication)
67. Vanderlinden E, Van Winkel N, Naesens L, Van Damme E, Persoons L, Schols D (2021) *In vitro* characterization of the carbohydrate-binding agents HHA, GNA, and UDA as inhibitors of influenza A and B virus replication. Antimicrob Agents Chemother 65:e01732-e1820. https://doi.org/10.1128/aac.01732-20
68. Vermeire K, Princen K, Hatse S, De Clercq E, Dey K, Bell TW, Schols D (2004) CADA, a novel CD4-targeted HIV inhibitor, is synergistic with various anti-HIV drugs in vitro. AIDS 18:2115–2125. https://doi.org/10.1097/00002030-200411050-00003
69. Skogman ME, Kanerva S, Manner S, Vuorela PM, Fallarero A (2016) Flavones as quorum sensing inhibitors identified by a newly optimized screening platform using *Chromobacterium*

violaceum as reporter bacteria. Molecules 21:1211. https://doi.org/10.3390/molecules21091211
70. Gopu V, Meena CK, Shetty PH (2015) Quercetin influences quorum sensing in food borne bacteria: in-vitro and in-silico evidence. PLoS ONE 10:e0134684. https://doi.org/10.1371/journal.pone.0134684
71. Guerin TF, Mondido M, McClenn B, Peasley B (2001) Application of resazurin for estimating abundance of contaminant-degrading microorganisms. Lett Appl Microbiol 32:340–345. https://doi.org/10.1046/j.1472-765X.2001.00916.x
72. Sandberg ME, Schellmann D, Brunhofer G, Erker T, Busygin I, Leino R, Vuorela PM, Fallarero A (2009) Pros and cons of using resazurin staining for quantification of viable *Staphylococcus aureus* biofilms in a screening assay. J Microbiol Methods 78:104–106. https://doi.org/10.1016/j.mimet.2009.04.014
73. Zhang JH, Chung TD, Oldenburg KR (1999) A simple statistical parameter for use in evaluation and validation of high throughput screening assays. J Biomol Screen 4:67–73. https://doi.org/10.1177/108705719900400206
74. Bollini S, Herbst JJ, Gaughan GT, Verdoorn TA, Ditta J, Dubowchik GM, Vinitsky AJ (2002) High-throughput fluorescence polarization method for identification of FKBP12 ligands. Biomol Screen 7:526–530. https://doi.org/10.1177/1087057102238626